European air quality maps of ozone and PM_{10} for 2006 and their uncertainty analysis

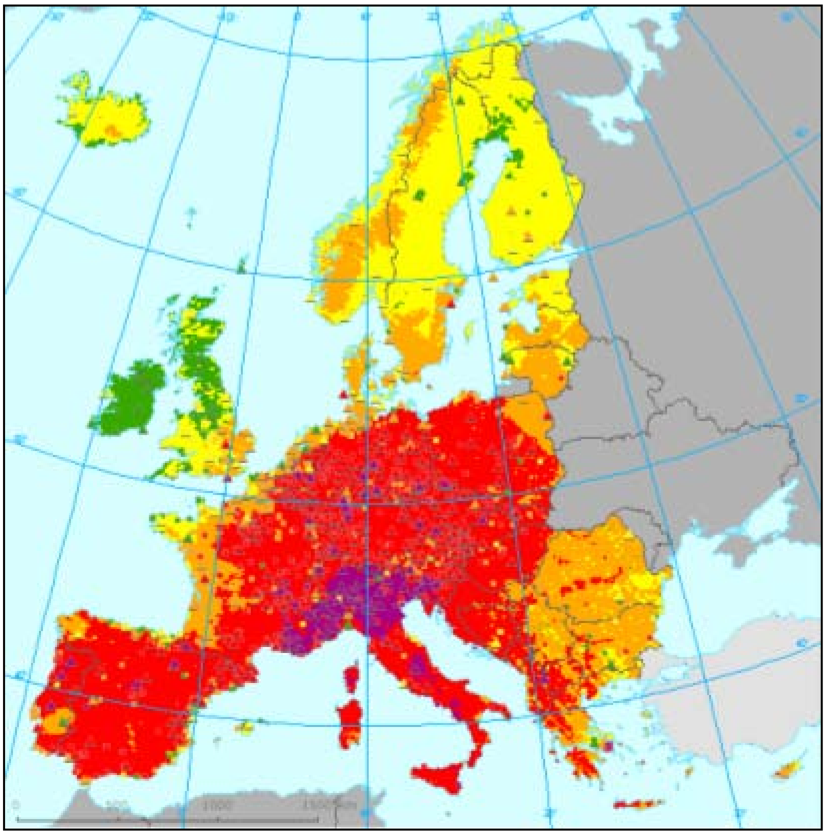

ETC/ACC Technical Paper 2008/8
February 2009

Peter de Smet, Jan Horálek, Markéta Coňková, Pavel Kurfürst, Frank de Leeuw, Bruce Denby

European Topic Centre
on Air and Climate Change

The European Topic Centre on Air and Climate Change (ETC/ACC)
is a consortium of European institutes under contract of the European Environmental Agency
PBL UBA-D UBA-V NILU AEAT AUTh CHMI MET.NO ÖKO TNO REC

Front page picture:
The ozone levels for the health indicators 26th highest daily maximum 8-hour value in µg.m^{-3} for both the rural and urban areas, combined into one final map for the year 2006. Its target value is 120 µg.m^{-3}. (Figure 5.1 of this paper). Note the considerable increase in the ozone levels above the target value compared to those of 2005 (as presented on the cover of ETC/ACC Technical Paper 2007/7).

Author affiliation:
Peter de Smet, Frank de Leeuw: Netherlands Environmental Assessment Agency (PBL), Bilthoven, The Netherlands
Jan Horálek, Markéta Coňková, Pavel Kurfürst: Czech Hydrometeorological Institute (CHMI), Praha, Czech Republic
Bruce Denby: Norwegian Institute of Air Research (NILU), Kjeller, Norway

DISCLAIMER

ETC/ACC Technical paper 2008/8
European Topic Centre on Air and Climate Change
PO Box 303
3720 AH Bilthoven
The Netherlands
Phone +31 30 2743550
Fax +31 30 2744433
Email etcacc@mnp.nl
Website http://air-climate.eionet.europa.eu/

Contents

1 Introduction

The objective of this paper is the updating of European air quality concentration maps, their exceedance probability and population exposure estimates based on interpolation of annual statistics of the 2006 observational data reported by EEA Member countries in 2007. The paper presents the mapping results and includes an uncertainty analysis of the interpolated maps, building upon methodological developments of earlier reports from Horálek et al. (2007, 2008).

The products of this work are mainly intended to be used for the assessment of European air quality by the EEA and its ETC/ACC, and for (interactive visual) public information purposes through the EEA website.

The two main pollutants of interest, PM_{10} and ozone, have been considered as relevant for an annual update and are dealt with in this paper. Mapping $PM_{2.5}$ is a theme dealt with in a separate ETC/ACC Technical Paper (De Leeuw, 2009).

The mapping methods applied are the same as recommended and described in Horálek et al. (2007, 2008). This includes that European-wide on a 10x10 km grid resolution, a rural interpolated map based on rural background measurements and an urban map based on urban and suburban background measurements are created separately, and subsequently a final combined map is derived by merging them together, using a weighing function based on the population density. Next to measured air quality data other supplementary data such as output from (currently) the Unified EMEP chemical transport model, altitude and several meteorological parameters are used in the mapping procedure. Depending on their level of contribution in improving the interpolation calculations we apply different supplementary parameters for each pollutant indicator type and each area type, following the recommendations of Horálek et al. (2008) of which EEA (2009a) is a derived report.

Next to annual indicator maps, we present the population exposure to PM_{10} and ozone and vegetation exposure for ozone.

For all the maps, we include a quantitative estimate of their interpolation uncertainty, using cross-validation parameters and scatter-plots. In addition, the paper contains the maps with probability estimates of limit/target value exceedances.

Chapter 2 describes briefly the used methodology. Chapter 3 documents all input data. Chapters 4 and 5 present the calculations, the mapping, the exposure and the uncertainty results for PM_{10} and ozone respectively. In Chapter 7 the overall conclusions are presented.

2 Used methodology

Some of the previously produced ETC/ACC Technical Papers (2007/7, 2006/6, 2005/8 and 2005/7) on the subject of spatial interpolation and its uncertainties do contain more methodological details and literature references than is summarised in this chapter.

2.1 Mapping method

The mapping method used is the linear regression model followed by the kriging of its residuals (residual kriging). The interpolation is carried out according to the relation:

$$\hat{Z}(s_0) = c + a_1.X_1(s_0) + a_2.X_2(s_0) + ... + \eta(s_0) \qquad (2.1)$$

where $\hat{Z}(s_0)$ is the estimated value of the air pollution indicator at the point s_o

$X_1(s_0), X_2(s_0), \ldots$ are the individual supplementary quantities at the point s_o

$c, a_1, a_2, \ldots$ are the parameters of the linear regression model calculated at the points of measurement,

$\eta(s_0)$ is the spatial interpolation of the residuals of the linear regression model at the points of measurement.

The spatial interpolation of residuals is carried out using ordinary kriging based on variogram estimates using a spherical function (with parameters: *nugget, sill, range*). For different pollutants and the area types (rural, urban), different supplementary data are used, depending on their contribution to improving the fit of the regression.

The maps are constructed separately for the rural and urban areas. The merging of the rural and urban maps into one combined air quality indicator map is done using a European-wide population density grid. For areas with population density less than the defined value of α_1, the rural map is applied, and for areas with a population density greater than the defined value α_2, the urban map is applied. For areas with population density within the interval (α_1, α_2) the weighting function of α_1 and α_2 is applied (see Horálek et al., 2005, 2007 and 2008).

The separate mapping of rural and urban areas and their subsequent merging is based on the presumption that in neighbouring locations, rural air pollution levels are lower (in case of PM_{10}), or higher (in case of ozone) than urban air pollution. This holds in general for most areas. However, it is not the case for several limited areas, of which the extent is between 4.5 % and 11.5 % of the total area in 2006, depending on the pollutant and indicator. For these cases a modification in the concentrations is computed on the basis of all background stations, both rural and (sub)urban, for the given pollutant resulting in an auxiliary field. For the areas where the rural field shows higher levels of air pollution in case of PM_{10}, or lower levels than the urban field in case of ozone, both rural and urban maps are modified according to the auxiliary field computed from all stations. The final merging of the resulting urban and rural maps is carried out by the application of the methodology described in Section 3.3 of Horálek et al. (2007), which uses the population density field. The value of the parameters α_1 and α_2 in its equation 3.2 are set again as α_1 = 100 inhbs.km^{-2} and α_2 = 500 inhbs.km^{-2} on the basis of the analysis presented in Horálek et al. (2005).

For detailed description of the used methods, see Horálek et al. (2007).

2.2 Calculation of population and vegetation exposure

Population exposure for individual countries and for Europe as a whole is calculated based on the air quality maps and population density data, both in EEA reference 10x10 km grid. For each concentration class, the total population per country as well as European-wide is determined. In addition, the population exposure per country and European-wide is expressed as the population-weighted concentration according equation:

$$\hat{c} = \frac{\sum_{i=1}^{N} c_i p_i}{\sum_{i=1}^{N} p_i} \tag{2.2}$$

where $\hat{c}$ is the average concentration per inhabitant in the country or in the whole of Europe,
p_i is the population in the i^{th} grid cell,
c_i is the concentration in the i^{th} grid cell,
N is the number of grid cells in the country or in Europe as a whole.

Vegetation exposure for individual countries and for Europe as a whole is calculated based on the air quality maps and land cover data, both in 2x2 km grid. For each concentration class, the total vegetation area per country as well as European-wide is determined.

2.3 Methods for uncertainty analysis

The first and basic method we use for uncertainty estimation of the European map is cross-validation. The cross-validation method computes the quality of the spatial interpolation for each measurement point using all the available information except from that one point, i.e. it withholds one data point and then makes a prediction at the spatial location of that point and this procedure is repeated for all measurement points of the available set. The predicted and measured values at these points are compared by drawing its scatter plot and with help of statistical indicators one indicates objectively the quality of the predictions. This method is quite exact – no suppositions are needed to be fulfilled. The advantage of the nature of this cross-validation technique is that it enables to evaluate the quality of the predicted values given in the resulting interpolation field at locations without measurements, though as long as they are within the area covered by the measurements.

In addition, we make a simple comparison between the point measurements and interpolated values of the 10 x 10 km grid which we apply for mapping the interpolation results. The 10x10 km grid value is the averaged result of the interpolations for that 10x10 km area. It means such grid cell will always have a value which represents an approximation of the predicted value(s) at the station(s) lying within that cell.

Another method we use is based on a geostatistical theory: together with the prediction, the prediction standard error is computed at all the grid cells, which represents in fact the interpolation uncertainty map (see details in Cressie, 1993). Based on the concentration and the uncertainty map the exceedance probability maps are created.

2.3.1 Cross-validation

The results of cross-validation are described by the statistical indicators and scatter plots. The main indicator used is root mean squared error (RMSE) and additional is the mean prediction error (MPE):

$$RMSE = \sqrt{\frac{1}{N}\sum_{i=1}^{N}(Z(s_i) - \hat{Z}(s_i))^2} \tag{2.3}$$

$$MPE = \frac{1}{N}\sum_{i=1}^{N}(Z(s_i) - \hat{Z}(s_i)) \tag{2.4}$$

where $Z(s_i)$ is the measured concentration at the i^{th} point, $i = 1, ..., N$,
$\hat{Z}(s_i)$ is the estimated concentration at the i^{th} point using other information, without the measured concentration at the i^{th} point,
N is the number of the measuring points.

RMSE should be as small as possible, MPE should be as close to zero as possible.

2.3.2 Comparison of the point measured and interpolated grid values

The comparison of measured and predicted grid values is described by the parameter and statistics values of the linear regression equation as well as the ordinary kriging variogram.

2.3.3 Exceedance probability mapping

The maps with the probability of exceedance (PoE) of a specific threshold value (e.g. limit or target value) are constructed using the concentration and uncertainty maps:

$$PoE(x) = 1 - \Phi\left(\frac{LV - C_c(x)}{\delta_c(x)}\right) \quad \text{(A.5)}$$

where $PoE(x)$ is the probability of limit/target value (*LV/TV*) exceedance in the grid cell *x*,
$\Phi()$ is the cumulative distribution function of the normal distribution,
LV is the limit or target value of the relevant indicator,
$C_c(x)$ is the estimated combined concentration value in the grid cell *x*,
$\delta_c(x)$ is the combined standard error of the estimation in the grid cell *x*.

And ultimately, the standard error of the probability map of the combined (rural and urban) map is calculated from the standard errors of the composing rural and urban maps, see Horálek et el. (2008).

3 Input data

Chapter 4 of Horálek et al. (2007) provides a complete overview on sources and specifications of the input data. For clarity and readability of this paper we provide here the full list of the used data. The key data is the air quality measurements at the point of stations. The supplementary data cover the whole area. All supplementary data were converted into the reference EEA LAEA5210 projection on a 10x10 km grid resolution, except for the AOT40 maps for which the data were converted into a 2x2 km grid resolution to allow for accurate land cover exposure estimates.

3.1 Measured air quality data

The air quality data were extracted from the European monitoring database AirBase, supplemented by several rural EMEP stations which are not reported to AirBase. Only data from stations classified by AirBase and/or EMEP as *rural*, *suburban* and *urban background* stations has been used. *Industrial* and *traffic* station types are not considered, since they represent local scale concentration levels not applicable at the mapping resolution employed. The following components and their indicators were considered:

PM_{10} – annual average [$\mu g.m^{-3}$], year 2006
– 36th maximum daily average value [$\mu g.m^{-3}$], year 2006

Ozone – 26th highest daily maximum 8-hour average value [$\mu g.m^{-3}$], year 2006
– SOMO35 [$\mu g.m^{-3}.day$], year 2006
– AOT40 for crops [$\mu g.m^{-3}.hour$], year 2006
– AOT40 for forests [$\mu g.m^{-3}.hour$], year 2006

SOMO35 is the annual sum of maximum daily 8-hour concentrations above 35 ppb (i.e. 70 $\mu g.m^{-3}$). AOT40 is the sum of the differences between hourly concentrations greater than 80 $\mu g.m^{-3}$ (i.e. 40 ppb) and 80 $\mu g.m^{-3}$, using only values measured between 7:00 and 19:00 UTC, calculated over the three months from May to July (AOT40 for crops), respectively over the six months from April to September (AOT40 for forests). Note that the term *vegetation* as used in the ozone directive is not further defined. Comparing the definitions in the Mapping Manual (UNECE, 2004) and those in the ozone directive suggests that we have to interpret the term *vegetation* in the ozone directive as agricultural crops. The exposure of *agricultural crops* has been evaluated here on basis of the AOT40 for vegetation as defined in the ozone directive.

In case of components affecting human health (i.e. PM_{10}, and the ozone parameters 26th highest daily maximum 8-hour average value and SOMO35) data from *rural*, *urban* and *suburban* background stations are considered. In case of components affecting vegetation (both AOT40 parameters for ozone) only *rural* background stations are considered.

Only the stations with annual data coverage of at least 75 percent are used. The stations from French overseas areas (departments) have been excluded. Additionally, the ozone station GR0110R and in the case of AOT40 also the station BG0053 with highly questionable data have been excluded from the analysis.

In addition to the AirBase data, 12 additional rural PM_{10} stations from the EMEP database have been used to reach a more extended spatial coverage by measurement data.

Table 3.1 shows the number of the measurement stations selected for the individual pollutants and their respective indicators.

Table 3.1 Number of the stations selected for the individual indicators and areas. For rural areas the rural background stations and for urban areas the urban and suburban background stations are used.

	PM10		ozone			
	annual average	36th daily maximum	26th highest daily max. 8h	SOMO35	AOT40 for crops	AOT40 for forests
rural	234	234	455	454	458	458
urban	849	849	892	892		

3.2 Unified EMEP model output

The established European chemical dispersion model used is the Unified EMEP model (revision rv3.0.5 for ozone and rv2.7.10 for PM_{10}), which is a Eulerian model with a resolution of 50 x 50 km. This model provides information at a 50x50 km scale; the disaggregation to the 10x10km grid cells is done as described in Section 4.4 of Horálek et al. (2007). Output from this model (2006 data extracted in October 2008) is used for the same parameter set as the set of measurement parameters in Section 3.1:

PM_{10} – annual average [$\mu g.m^{-3}$], year 2006
– 36^{th} maximum daily average value [$\mu g.m^{-3}$], year 2006

Ozone – 26^{th} highest daily maximum 8-hour average value [$\mu g.m^{-3}$], year 2006
– SOMO35 [$\mu g.m^{-3}.day$], year 2006
– AOT40 for crops [$\mu g.m^{-3}.hour$], year 2006
– AOT40 for forests [$\mu g.m^{-3}.hour$], year 2006

The model is described by Simpson et al. (2003), Fagerli et al. (2004) and at the web site http://www.emep.int/OpenSource/index.html. The model results are based on the emissions for the relevant year (Vestreng et al., 2007) and actual meteorological data (from PARLAM-PS, i.e. special dedicated 2000 version of HIRLAM numerical weather prediction model, with parallel architecture, see Sandnes Lenschow and Tsyro, 2000). Details on the EMEP modelling with the 2006 data are given for ozone by Tarrasón and Nyíri (2008) and for PM_{10} by EMEP (2008).

In the case of ozone parameter 26^{th} highest daily maximum 8-hour average value we did not obtain the modelled data for Iceland and Jan Mayen. The missing modelled data were estimated from the modelled SOMO35 data for the relevant areas, using linear regression between modelled data for SOMO35 and 26^{th} highest daily maximum 8-hour average value.

3.3 Altitude

We used the European covering altitude data field (in meters) of GTOPO30, original grid resolution of 30 x 30 arcsec. For details, see Horálek et al (2007).

3.4 Meteorological parameters

Actual meteorological surface layer parameters are extracted from the Meteorological Archival and Retrieval System (MARS) of the ECMWF (European Centre for Medium-range Weather Forecasts). The derived parameters currently used extracted from the ECMWF variables, specified in detail in Horálek et al. (2007) Section 4.5, are:

Wind speed – annual average [$m.s^{-1}$], year 2006
Surface solar radiation – annual average [$MWs.m^{-2}$], year 2006

3.5 Population density

Population density [$inhbs.km^{-2}$] is based on JRC data for the majority countries (Source EEA, pop01c00v3int, official version Aug. 2006; Owner: JRC). For countries (Andorra, Albania, Bosnia-Herzegovina, Cyprus, Iceland, Liechtenstein, FYR of Macedonia, Montenegro, Norway, Serbia, Switzerland, and Turkey) and regions (Faroe Islands, Jersey, Guernsey, Man and Rhodos) which are not included in this map we used population density data from an alternative source, namely the ORNL LandScan (2002) Global Population Dataset. However, these data were not available for the southern part of Cyprus.

JRC data are spatially aggregated into EEA 10x10 km grid (contrary to the previous years, when a more complicated and less exact approach was used, see Horálek et al., 2007, Section 4.9).

ORNL data is spatially aggregated into EEA 10x10 km grid based on original non-smoothed data, contrary to the previous years when the smoothed ORNL data has been used. The data is compared on the one hand with JRC data for the countries covered by both population density data sources, and on the other hand with UN population (http://www.un.org/popin/data.html) for the individual countries. Based on these comparisons, which shows good agreement of JRC and UN data, but underestimation of ORNL data, a multiplication factor 1.5 was applied for all ORNL data. The difference with the previously used factor of 1.65 has its cause in the use of non-smoothed ORNL data. Figure 3.1 presents this comparison between JRC and ORNL data based on the national population totals of the individual countries.

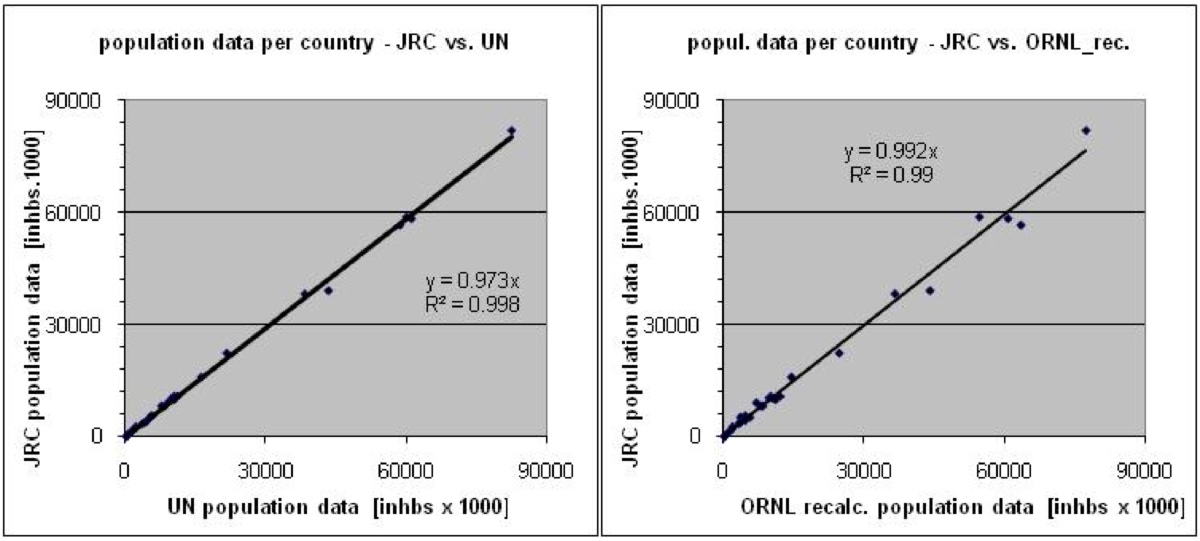

Figure 3.1 Correlation between JRC (y-axis) and UN (x-axis, left), respectively ORNL recalculated (x-axis, right) national population totals. The ORNL data is recalculated by multiplication factor 1.5.

Because of the above mentioned changes, slightly different population numbers per countries and for Europe as a whole are presented in the exposure tables in Chapters 4 and 5, compared to the numbers in Horálek et al.(2008).

3.6 Land cover

The input data from CORINE Land Cover 2000 (CLC2000) – grid 250 x 250 m, version 8/2005 version 2, (Source and owner: EEA, lceugr250_00) is used. The countries missing in this database are Iceland, Montenegro, Norway, Serbia, Switzerland, and Turkey.

In an effort to reduce the time demanding calculations on the large data quantity involved with the 250 x 250 m grid resolution an aggregation to a 500 x 500 m grid resolution is performed first, before the exceedance mapping and table extraction takes place. The ultimate map and table results are not influenced by this resolution aggregation.

4 PM_{10} maps

For PM_{10} the two health-related indicators annual average and 36th highest maximum daily average are considered. The maps were created using the combination of rural and urban areas, as described in Chapter 2. All the maps are constructed in the EEA LAEA5210 10x10 km grid.

4.1 Annual average

4.1.1 Concentration map

The combined interpolated map for the 2006 PM_{10} annual averages is created by combining the rural and urban maps using a 10x10 km grid aggregated population density field, according the criterion as described in Section 2 and in Horálek et al. (2007). Both rural and urban maps were created by combining the annual averages from the measured PM_{10} concentrations with supplementary data in a linear regression model, followed by the interpolation of its residuals by ordinary kriging.

The supplementary data were used in accordance with the recommendations given by Horálek et al. (2008). The recommended supplementary data for rural areas are EMEP model output, altitude, wind speed and surface solar radiation; for urban areas it is EMEP model output. (The relevant linear regression submodels are identified as P.Eawr and UP.E, respectively).

The estimated parameters of the linear regression models (*c*, a_1, a_2, ...) and of the residual kriging (*nugget, sill, range*) are presented in Table 4.1, including the statistical indicators of both the regression and the kriging. The R^2 and standard error are indicators for the closeness of the regression relation, where R^2 should be as close to 1 as possible and the standard error should be as small as possible. The table values for the adjusted R^2 of 0.29 for the rural areas and 0.03 for the urban areas show a closeness of the regression of similar level for the year 2005 with a value of 0.28 and 0.06 respectively (see Horálek et al. 2008, Tables A2.1, resp. A2.6). Over the years the low values for urban areas indicate that the closeness of the regression in urban areas is very poor (Horálek et al. 2007, 2008). RMSE and MPE are the cross-validation indicators, showing the quality of the resulting map, where RMSE should be as small as possible and MPE should be as close zero as possible. The MPE indicates to what extend the estimation is un-biased. More detailed analysis and comparison with 2005 results is given in Section 4.1.3.

Table 4.1 Parameters of the linear regression models (c, a1, a2, ...) and of the ordinary kriging variograms (nugget, sill, range) - and their statistics - of PM_{10} indicator annual average for 2006 in the rural (left) and rural (right) areas as used for the final combined map, i.e. rural linear regression model P.Eawr (left), resp. urban UP.E (right) followed by interpolation on its regression residuals using ordinary kriging (OK, coded with ‘a’).

linear regr. model + OK on its residuals	rural areas (P.Eawr-a)	urban areas (UP.E-a)
	coeff.	coeff.
c (constant)	30.2	22.6
a1 (EMEP model 2006)	1.19	0.70
a2 (altitude GTOPO)	-0.0096	
a3 (wind speed 2006)	-4.50	
a4 (s. solar radiation 2006)	non significant	
adjusted R^2	**0.29**	**0.03**
standard error [µg.m^{-3}]	**7.02**	**10.95**
nugget	15	21
sill	34	85
range [km]	210	390
RMSE [µg.m^{-3}]	**5.79**	**6.09**
MPE [µg.m^{-3}]	**0.09**	**0.07**

The final map is presented in Figure 4.1. The areas and stations in the combined map where the limit value (LV) of 40 µg.m^{-3} is exceeded are coloured red and purple.

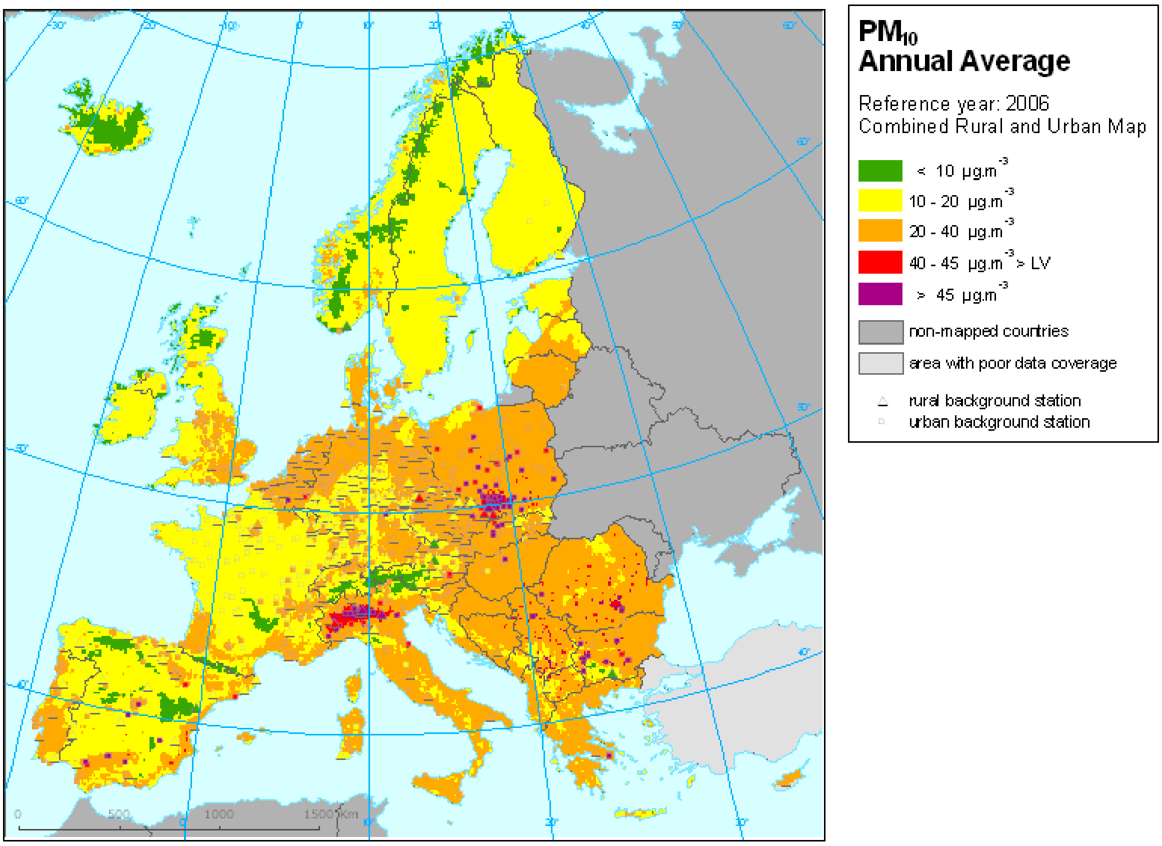

Figure 4.1 Combined rural and urban concentration map of PM_{10} – annual average, year 2006. Spatial interpolated concentration field and the measured values in the measuring points. Units: µg.m^{-3}.

4.1.2 Population exposure

Table 4.2 gives the population frequency distribution for a limited number of exposure classes, as well as the population-weighted concentration for individual countries and for Europe as a whole according Equation 2.2.

Table 4.2 Population exposure and population weighted concentration – PM_{10}, annual average, year 2006

Country	Population	2006 Percent [%]					Population weighted conc.
	x1000	< 10 $\mu g.m^{-3}$	10 - 20 $\mu g.m^{-3}$	(< LV) 20 - 40 $\mu g.m^{-3}$	(> LV) 40 - 45 $\mu g.m^{-3}$	> 45 $\mu g.m^{-3}$	[$\mu g.m^{-3}$]
Austria	8217	2.7	21.2	76.1	0	0	23.8
Belgium	10594	0	2.2	97.8	0	0	30.9
Bulgaria	8011	0.3	4.2	63.3	4.8	27.5	36.7
Croatia	4400	0	3.1	96.9	0	0	29.9
Czech Republic	10163	0	4.6	84.8	3.2	7.4	31.7
Denmark	5423	0.9	17.0	82.1	0	0	22.3
Estonia	1364	1.7	55.7	42.6	0	0	18.8
Finland	5184	3.5	91.4	5.1	0	0	16.6
France	58437	0.3	53.3	46.4	0	0	20.1
Germany	82028	0.0	18.4	81.6	0	0	23.1
Greece	10876	0.0	6.3	93.2	0.4	0	31.7
Hungary	10125	0	0	99.0	1.0	0	32.5
Ireland	3734	7.0	93.0	0	0	0	13.8
Italy	56675	0.3	3.5	73.9	7.6	14.6	32.8
Latvia	2390	0.2	29.2	70.5	0	0	21.5
Liechtenstein	35	0	38.3	61.7	0	0	21.6
Lithuania	3479	0	6.6	93.4	0	0	22.3
Luxembourg	427	0	20.2	79.8	0	0	20.3
Malta	395	0	0	100.0	0	0	28.7
Netherlands	15746	0	0.2	99.8	0	0	28.9
Poland	38237	0	2.2	76.7	5.9	15.2	34.4
Portugal	9910	0.0	18.8	81.2	0	0	27.3
Romania	22341	0	1.3	66.8	10.4	21.4	36.2
San Marino	20	0	0	100.0	0	0	27.7
Slovakia	5295	3.0	90.9	5.0	1.1	0	30.8
Slovenia	2047	0.0	10.3	89.7	0	0	26.9
Spain	39046	0.9	20.9	75.5	2.4	0.2	28.0
Sweden	8898	2.1	87.9	10.0	0	0	17.4
United Kingdom	59051	0.8	16.6	82.6	0	0	22.5
Albania	3961	0	9.4	89.5	1.1	0	30.3
Andorra	61	33.3	0	66.7	0	0	18.1
Bosnia-Herzegovina	4203	0	2.3	92.5	5.1	0	31.4
Iceland	183	13.4	81.2	5.4	0	0	15.4
Macedonia, F.Y.R. of	2297	0	7.9	40.4	16.2	35.5	37.5
Montenegro	724	0	18.6	81.4	0	0	28.2
Norway	3226	5.8	46.6	47.6	0	0	18.8
Serbia	10821	0	2.2	48.3	10.7	38.7	38.7
Switzerland	7270	1.3	17.7	81.0	0	0	21.8
Total	**515294**	**0.5**	**19.5**	**72.3**	**2.4**	**5.2**	**27.1**
Total		**20.0**			**7.7**		

Note: Countries with the values based on ORNL population data with uncertain quality: AD, AL, BA, CH, IS, ME, MK, NO, RS. Countries with the lack of air quality or population density data are excluded from calculations in this paper: CY, TR.

About one fifth (20 %) of the European population is exposed to concentrations below 20 $\mu g.m^{-3}$. In 2006 more than two-third (72.3 %) of the European population lives in areas where the PM_{10} concentration is estimated at being between 20 and 40 $\mu g.m^{-3}$. About 8 % of the population lives in areas where the PM_{10} annual limit value is exceeded. However, as the next section discusses the current mapping methodology tends to underestimate high values, thus the percentage will most likely be higher. The frequency distribution shows a large variability over Europe; in six countries (Bulgaria, FYR of Macedonia, Italy, Poland, Romania, and Serbia) it is estimated that more than one fifth of the population is exposed to concentrations above the limit value. In a number of countries in north and north-west Europe the LV of 40 $\mu g.m^{-3}$ seems not to be exceeded at the 10x10 km level applied in the mapping. In comparison with the year 2005, more people are exposed to the concentrations between

20 and 40 µg.m^{-3} (67 % in 2005), while less people live in areas above the LV (9 % in 2005) and below 20 µg.m^{-3} (24 % in 2005).

It is estimated that the European inhabitants living in the background (i.e. neither hot-spot nor industrial) areas – without regard whether urban or rural – are exposed on average to the annual mean PM_{10} concentration of 27 µg.m^{-3}. In comparison with 2005 the overall European population-weighted concentration is about 1 µg.m^{-3} higher in 2006.

4.1.3 Uncertainties

Uncertainty estimated by cross-validation

The basic uncertainty analysis is given by cross-validation. Using RMSE as the most common indicator, the *absolute mean uncertainty* of the maps in positions without measurement within the areas covered by measurements - i.e. excluding areas lacking monitoring stations such as the Balkan - can be expressed in µg.m^{-3}. Table 4.1 shows that the absolute mean uncertainty of the combined map of PM_{10} annual average expressed by RMSE is 5.8 µg.m^{-3} for the rural areas and 6.1 µg.m^{-3} for the urban areas. In 2005 the RMSE values were 5.5 µg.m^{-3} for both, meaning the map for 2006 shows a somewhat higher level of absolute mean uncertainty than the map for 2005.

Alternatively, this uncertainty can be expressed as the absolute RMSE uncertainty being a percentage of the mean air pollution indicator value for all stations. This *relative mean uncertainty* of the map of PM_{10} annual average is 26.6 % for rural areas and 20.9 % for urban areas and just slightly higher, 0.7 %, resp. 0.9 %, than the uncertainties of the 2005 map. The higher percentages have probably their cause in a poorer fit of the linear regression. For example, compared to the 2005 results in Horálek et al., (2008) where *c* was 19 and *nugget* was 15 in the urban areas, Table 4.1 shows for 2006 at the urban areas a higher intercept *c* probably causing the higher nugget in the interpolation. However, these relative uncertainty values are still quite good results in comparison with the requirement of the maximum relative uncertainty at the level of 50 % for the modelling of PM_{10} annual average according to the Annex VIII of the first air quality daughter directive.

Figure 4.2 shows the cross-validation scatter plots, obtained according Section 2.3, for both the rural and urban areas. The R^2 indicates that for the rural areas about 52 % and for the urban areas about 69 % of the variability is attributable to the interpolation. The values for the 2005 map were 52 % and 71 % respectively, showing a similar level of performance for the rural interpolations at both years, while the interpolation performance at the 2006 urban areas is just a slightly poorer compared to 2005.

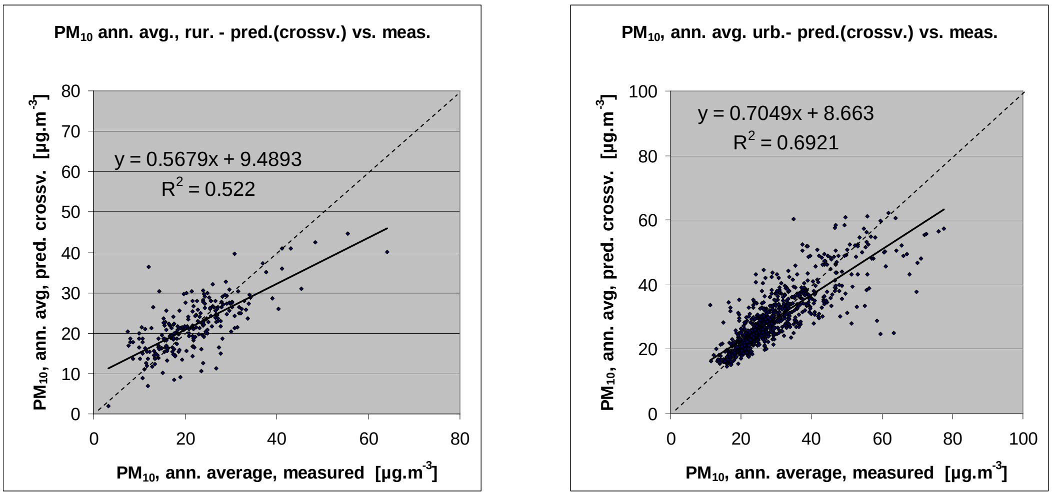

Figure 4.2 Correlation between cross-validation predicted values (y-axis) and measurements (x-axis) for the PM_{10} annual average for 2006 for rural (left) and urban (right) areas. R^2 and the slope a (from the linear regression equation $y = a \cdot x + c$) should be as close 1 as possible, the intercept c should be as close 0 as possible

The scatter plots show that at areas with high values there will be a level of underestimation that leads to predicted interpolated values being too low at locations without measurements. For example, at urban areas without a station the value of 60 µg.m^{-3} will be estimated on average at about 50 µg.m^{-3} only, which is about 15 % too low. This underestimation at high values is natural to all spatial interpolations. It can be reduced by either using a higher number of the stations, or introducing a closer regression by using some other supplementary data.

Comparison of point measurement values with the predicted grid value

Additional to the above point cross-validation, a simple comparison between the point measured and interpolated values averaged in a 10x10 km grid has been made. This point-grid value comparison indicates to what extend the predicted value of a grid cell represents the corresponding measured station values covered by that cell. The results of the point cross-validation compared to this point-grid validation examination are summarised in Table 4.3. The table shows a better correlated relation between station measurements and the interpolated values of the corresponding grid cells for both rural and urban areas (i.e. higher R^2, smaller intercept and the slope closer to 1) than it does at the point cross-validation predictions of Figure 4.2. This has its cause in the fact that the simple comparison between points measurements and gridded interpolated values shows the uncertainty at the actual station locations (points) itself, while the cross-validation simulates the behaviour of the interpolation at positions without actual measurements within the area covered by measurements. The uncertainty at measurement locations is caused partly by the smoothing effect of the interpolation and partly by the spatial averaging of the values in the 10x10 km grid cells. The level of the smoothing effect leading to underestimation at high values is there smaller than it is at areas without measurement. For example, in the case of urban areas the predicted interpolation gridded value will be about 50 µg.m^{-3} at the corresponding station point with the measured value of 55 µg.m^{-3}.

Table 4.3 Linear regression equation and coefficient of determination R^2 from the scatter plots of (i) the predicted point values based on cross-validation and (ii) the aggregated predictions into 10x10 km grid cells versus the measured point values for PM_{10} indicator annual average for rural and urban areas.

	rural areas		urban areas	
	equation	R^2	equation	R^2
i) cross-validation prediction	y = 0.568x + 9.49	0.522	y = 0.705x + 8.66	0.692
ii) 10x10 km grid prediction	y = 0.776x + 4.89	0.891	y = 0.804x + 5.73	0.869

Probability of limit value exceedance map

Next to the cross-validation analysis and the comparison of predicted grid values with the points of measurement, the map with the probability of the limit value exceedance has been constructed, using the concentration maps (Figure 4.1), the uncertainty map and the limit value (40 µg.m^{-3} for the annual average). The probability map is presented in Figure 4.3. Areas with a probability of limit value exceedance above 75 % are marked in red, meaning a *considerable* likelihood of exceedance; areas below 25 % are marked in green and show a *low* likelihood of exceedance. The red areas indicate areas for which exceedance may occur very likely due to either high concentrations close to or already above the LV including such enclosed uncertainty that exceedance is very likely, or the red areas indicate lower concentrations with such high uncertainty levels reaching above the LV that exceedance is very likely. Vice versa, in the green areas it is not very likely to have prediction values showing exceedance and/or such enclosed uncertainties that reaching above the LV is not very likely.

Areas with 25-50 %, resp. 50-75 % probability of LV exceedance are marked in yellow and orange. The yellow colour indicates the areas with the estimated values below limit value for which there exists a *moderate* chance of exceeding the limit. Contrary, the orange areas are above the limit value according to estimation, but with a chance of non exceedance caused by the uncertainty of the estimation, i.e. a *reasonable* likelihood of exceedance. The patterns in the spatial distribution of the different probability classes over Europe do not differ much from those of 2005; just some enlargement and shift in the isolated yellow spots with a moderate likelihood of exceedance in the south-eastern countries of Europe where relative little measurement stations are located.

In the areas where exceedances are observed, such as the Po Valley and the south of Poland, there the probability of exceedances are also the highest, meaning that in these areas reasonable reductions may be needed to reach non-exceedance levels in the future.

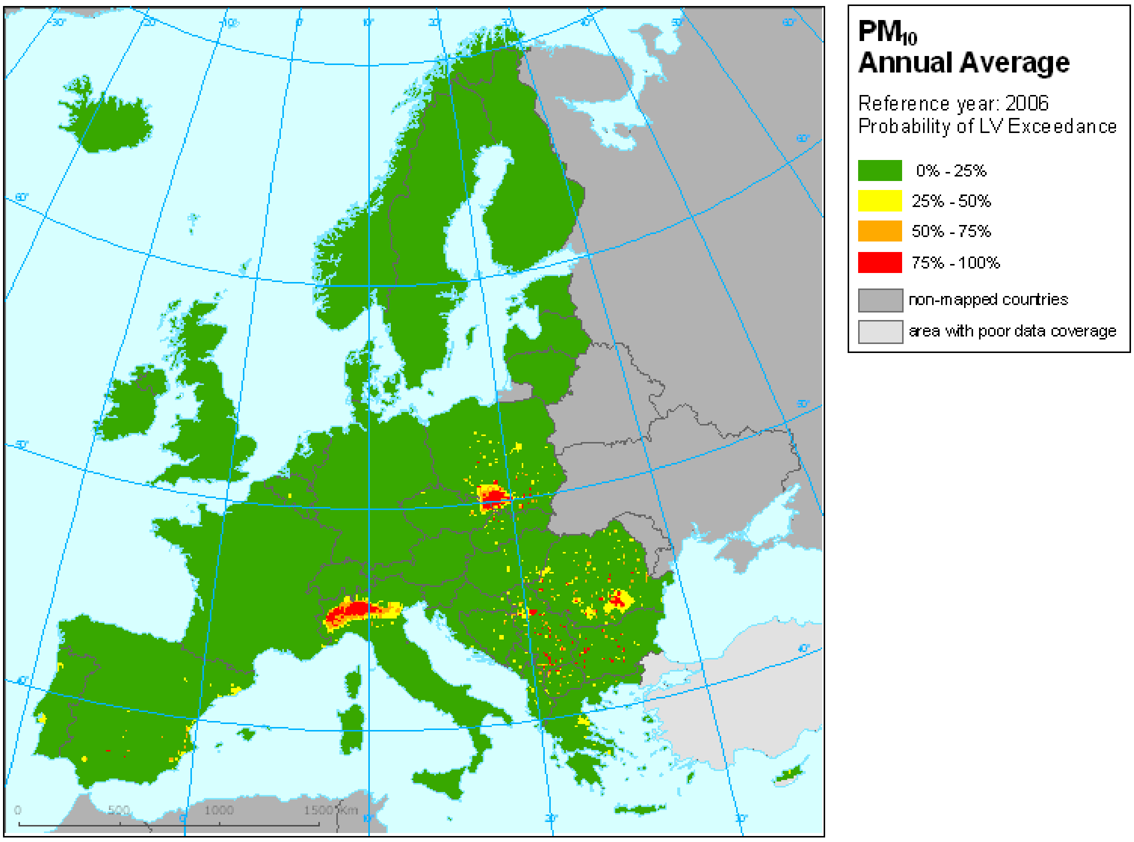

Figure 4.3 Map with the probability of the limit value exceedance for PM_{10} annual average for 2006, in $\mu g.m^{-3}$ on the European scale on the 10 x 10 km grid resolution. Interpolation uncertainty only is considered, no other sources of uncertainty.

4.2 36th highest daily average

4.2.1 Concentration map

Like in the case of PM_{10} annual average, also for 36th highest daily value the combined interpolated map is created by combining the rural and urban maps, according the criterion as described in Section 2 and in Horálek et al. (2007). Both rural and urban maps were created by combining the annual averages from the measured PM_{10} concentrations with supplementary data in a linear regression model, followed by the interpolation of its residuals by ordinary kriging.

The recommended supplementary data given by Horálek et al. (2008) are the same as for annual average, i.e. EMEP model output, altitude, wind speed and surface solar radiation for rural areas and EMEP model output for urban areas. (The relevant linear regression submodels are identified as P.Eawr and UP.E respectively).

The estimated parameters of the linear regression models and of the residual kriging are presented in Table 4.4, including the statistical indicators for both the linear regression models and the residual kriging.

Table 4.4 Parameters of the linear regression models (c, a1, a2, …) and of the ordinary kriging variograms (nugget, sill, range) - and their statistics - of PM_{10} indicator 36^{th} maximum daily mean for 2006 in the rural (left) and rural (right) areas as used for final mapping, i.e. rural linear regression model P.Eawr (left), resp. urban UP.E (right) followed by the interpolation on its regression residuals using ordinary kriging (OK, coded with 'a').

linear regr. model + OK on its residuals	rural areas (P.Eawr-a)	urban areas (UP.E-a)
	coeff.	coeff.
c (constant)	44.12	39.75
a1 (EMEP model 2006)	1.04	0.51
a2 (altitude GTOPO)	-0.015	
a3 (wind speed 2006)	-8.06	
a4 (s. solar radiation 2006)	0.66	
adjusted R^2	**0.27**	**0.02**
standard error [μg.m^{-3}]	**12.58**	**20.82**
nugget	37	98
sill	143	310
range [km]	220	400
RMSE [μg.m^{-3}]	**9.85**	**11.67**
MPE [μg.m^{-3}]	**0.22**	**0.13**

The R^2 and standard error show the closeness of the regression relation. The regressions on the 2006 data have an adjusted R^2 of 0.27 for the rural areas and 0.02 for the urban areas. This closeness is a slightly worse than in the year 2005, where the adjusted R^2 was 0.29 for rural areas and 0.06 for urban areas (see Horálek et al. 2008, Tables A2.1, resp. A2.6). Furthermore, the higher constant intercept *c* and lower slope a_1 in the year 2006 indicate a worse closeness in both the rural and urban areas (in 2005 the *c* and a_1 were 19.2, resp. 1.11 for rural areas, and 28.2, resp. 0.85 for urban areas, Horálek et al. 2008, Tables A2.4, resp. A2.10). RMSE and MPE are the cross-validation indicators for the quality of the resulting map. The RMSE analysis and comparison with 2005 results is discussed in Section 4.2.3.

The final map is presented in Figure 4.4. The areas and stations in the combined map where the limit value (LV) of 50 μg.m^{-3} is exceeded are coloured red and purple.

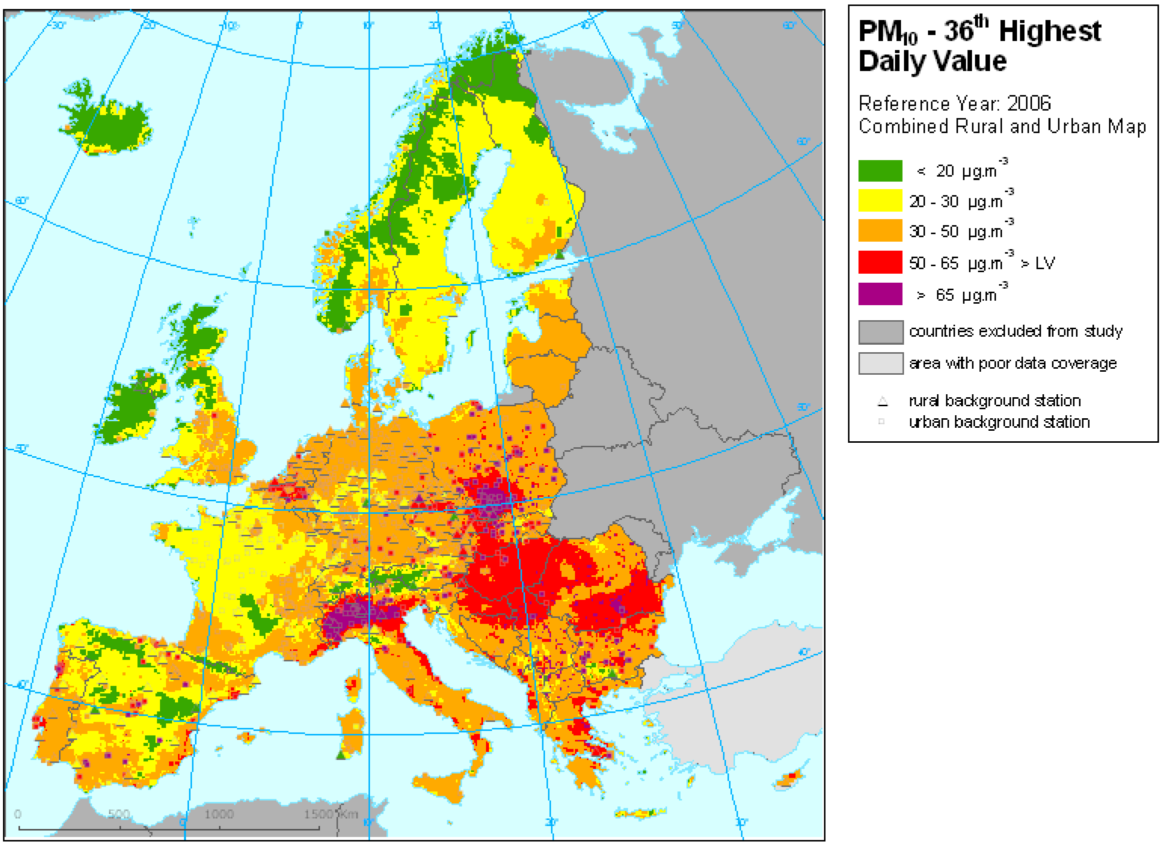

Figure 4.4 Combined rural and urban concentration map of PM_{10} – 36^{th} maximum daily average value, year 2006. Units: $\mu g.m^{-3}$.

4.2.2 Population exposure

Table 4.5 gives the population frequency distribution for a limited number of exposure classes, as well as the population-weighted concentration, for individual countries and for Europe as a whole.

Table 4.5 Population exposure and population weighted concentration – PM_{10}, 36th maximum daily average value, year 2006.

Country	Population x1000	2006 Percent [%] < 20 µg.m-3	20 - 30 µg.m-3	(< LV) 30 - 50 µg.m-3	(> LV) 50 - 65 µg.m-3	> 65 µg.m-3	Population-weighted conc. [µg.m-3]
Austria	8217	2.5	9.7	56.6	31.2	0	43.2
Belgium	10594	0	0.5	30.3	69.2	0	50.8
Bulgaria	8011	0.3	2.0	32.0	31.4	34.3	64.5
Croatia	4400	0.1	1.7	31.0	67.1	0	50.9
Czech Republic	10163	0	1.0	36.3	49.3	13.4	54.6
Denmark	5423	3.4	13.5	83.1	0	0	35.2
Estonia	1364	3.9	20.6	75.5	0	0	32.5
Finland	5184	6.5	52.0	41.6	0	0	28.5
France	58437	1.5	35.6	61.3	1.6	0	32.6
Germany	82028	0.0	4.9	94.0	1.1	0	39.7
Greece	10876	0.7	3.8	30.6	62.1	2.8	51.1
Hungary	10125	5.4	84.4	10.1	0	0	57.7
Ireland	3734	49.5	44.7	5.8	0	0	21.5
Italy	56675	0.3	2.0	44.6	26.6	26.5	56.9
Latvia	2390	1.2	2.3	96.5	0	0	39.0
Liechtenstein	35	0	0	100.0	0	0	42.4
Lithuania	3479	0.1	2.4	97.5	0	0	39.1
Luxembourg	427	0	1.6	98.4	0	0	35.0
Malta	395	0	0	100.0	0	0	44.0
Netherlands	15746	0	0.1	97.8	2.0	0	45.8
Poland	38237	0.0	0.8	39.4	33.2	26.6	59.4
Portugal	9910	0.0	8.3	41.6	50.0	0	46.1
Romania	22341	0	0.2	17.4	43.2	39.2	61.0
San Marino	20	0	0	100.0	0	0	46.7
Slovakia	5295	0	1.2	32.3	56.7	9.7	53.0
Slovenia	2047	0.1	4.7	52.3	42.8	0	45.6
Spain	39046	1.8	12.8	44.8	39.9	0.8	44.7
Sweden	8898	8.4	52.2	39.4	0	0	28.6
United Kingdom	59051	3.7	11.4	84.9	0	0	34.4
Albania	3961	0.0	3.5	33.4	58.7	4.5	51.3
Andorra	61	33.3	0	66.7	0	0	29.5
Bosnia-Herzegovina	4203	0	0.1	30.3	49.5	20.1	54.3
Iceland	183	38.9	27.9	33.1	0.1	0	23.4
Macedonia, F.Y.R. of	2297	0.2	2.0	29.9	3.0	64.9	66.6
Montenegro	724	0	9.3	46.1	19.6	24.9	49.1
Norway	3226	13.9	20.4	65.7	0	0	30.3
Serbia	10821	0	0.8	18.7	28.4	52.1	67.3
Switzerland	7270	0.7	7.2	88.1	3.4	0.7	41.4
Total	**515294**	**1.7**	**11.8**	**58.0**	**19.2**	**9.2**	**45.4**
			71.5		**28.5**		

Note: Countries with the values based on ORNL population data with uncertain quality: AD, AL, BA, CH, IS, ME, MK, NO, RS. Countries with the lack of air quality or population density data are excluded from calculations in this paper: CY, TR.

It is estimated that about 28 % of the population lives in areas where the PM_{10} limit value (50 µg.m^{-3}) of 36th maximum daily mean is exceeded. However, as the current mapping methodology tends to underestimate high values, this percentage will most likely be higher. The percentage of the population living in areas above the LV is similar to that of 2005.

The overall European population-weighted concentration of the 36th maximum daily mean for the background (i.e. neither hot-spot nor industrial) areas is estimated at about 45 µg.m^{-3}. Compared to the 2005 results in Horálek et al. (2008) it is just about 1.5 µg.m^{-3} higher in 2006.

4.2.3 Uncertainties

Uncertainty estimated by cross-validation

At first, the cross-validation analysis is executed. Using RMSE as the most common indicator, the absolute mean uncertainty of the maps in positions without measurement within the areas covered by measurements can be expressed in $\mu g.m^{-3}$. In Table 4.4 the absolute mean uncertainty of the combined map of PM_{10} indicator 36th highest daily mean expressed by RMSE is 9.8 $\mu g.m^{-3}$ for the rural areas and 11.7 $\mu g.m^{-3}$ for the urban areas. For the 2005 maps the RMSE values were 9.7 and 9.9 $\mu g.m^{-3}$ respectively, meaning the rural maps for both years show a similar level of absolute mean uncertainty while the urban map for 2006 shows a higher absolute uncertainty than for 2005.

Alternatively, this uncertainty can be expressed as the absolute RMSE uncertainty being a percentage of the mean air pollution indicator value for all stations. This relative mean uncertainty of the map of PM_{10} indicator 36th highest daily mean is 26.6 % for rural areas and 23.5 % for urban areas. Compared to the 2005 map with relative uncertainties of 26.3 % for rural areas and 21.4 % for urban areas, the relative uncertainty in the 2006 maps is the same for the rural areas and a slightly higher at the urban areas.

Figure 4.5 shows the cross-validation scatter plots for both rural and urban areas. The R^2 indicates that for the rural areas about 56 % and for the urban areas about 68 % of the variability is attributable to the interpolation. The values for the 2005 map were 55 % and 75 % respectively, showing a similar interpolation performance at the rural areas for both years, while the interpolation at the urban areas shows a poorer level of performance for the year 2006. This poorer level in urban areas is probably caused by the higher *nugget* value of 98 (Table 4.4) compared to the 2005 result, where the *nugget* was 45. The higher nugget may have its cause in a worse closeness of linear regression (Section 4.2.1).

The scatter plots show that at areas with high values the predicted interpolated values lead to an underestimation of the PM_{10} indicator at locations without measurements. For example, at urban areas the value of 80 $\mu g.m^{-3}$ will be estimated on average at about 70 $\mu g.m^{-3}$ only, which is more than 10 % too low.

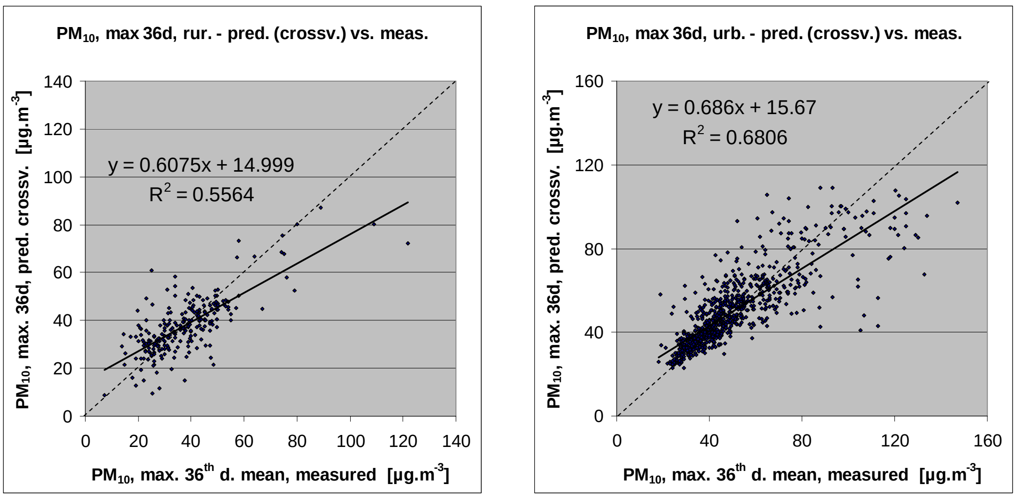

Figure 4.5 Correlation between cross-validation predicted values (y-axis) and measurements (x-axis) for the PM_{10} annual average for 2006 for rural (left) and urban (right) areas. R^2 and the slope a (from the linear regression equation $y = a \cdot x + c$) should be as close 1 as possible, the intercept c should be as close 0 as possible

Comparison of point measurement values with the predicted grid value

Additional to the cross-validation, a simple comparison between the measured and interpolated values averaged in a 10x10 km grid has been made. This point-grid comparison shows to what extend the predicted value of a grid cell represents the corresponding measured values covered by that cell. The results of the cross-validation compared to this gridded validation examination are summarised in Table 4.6. The uncertainty at measurement locations is caused partly by the smoothing effect of the interpolation and partly by the spatial averaging of the values in the 10x10 km grid cells. The level of the smoothing leading to underestimation at high values is here smaller than it is at areas without measurement: For example, in the case of urban areas the predicted interpolation gridded value will be about 70 µg.m^{-3} at the corresponding station point with the measurement value of 75 µg.m^{-3}

Table 4.6 Linear regression equation and coefficient of determination R^2 from the scatter plots of (i) the predicted point values based on cross-validation and (ii) the aggregation into 10x10 km grid cells versus the measured point values for PM_{10} indicator 36th maximum daily mean for rural and urban areas.

	rural areas		urban areas	
	equation	R^2	equation	R^2
i) cross-validation prediction	y = 0.608x + 15.00	0.556	y = 0.686x + 15.67	0.681
ii) 10x10 km grid prediction	y = 0.818x + 6.89	0.923	y = 0.769x + 11.45	0.840

Probability of limit value exceedance map

Next to the cross-validation analysis and the comparison of predicted grid values with the points of measurement, the map with the probability of the limit value exceedance has been constructed, using the concentration maps (Figure 4.4), the uncertainty map and the limit value (LV), defined in the directive as 50 µg.m^{-3} for the 36th highest daily mean. The probability map is presented in Figure 4.6. Areas with the probability of limit value exceedance above 75 % are marked in red (a *considerable* likelihood of exceedance); areas below 25 % are marked in green (*low*). Areas with 25-50 %, resp. 50-75 % probability of LV exceedance are marked in yellow (*moderate*) and orange (*reasonable*). Section 4.1.3 explains in more detail the significance of the colour classes in the map.

Comparing the 2005 with the 2006 probability of exceedance (PoE), one can conclude that in 2006 most of the Iberian Peninsula shows that the yellow contribution has turned into green. It means hardly any probability of exceedance resides, indicating that policy targets are or may be reached for these areas. Also reductions of relevance are observed in the Black Triangle, whereas in Denmark, north-eastern Poland, Latvia, Norway, and at coastal areas of Greece the PoE increased from low (green) to moderate (yellow). Of more concern are the increases observed in Hungary, Romania, Bulgaria, Balkan areas, east-coast of Italy, and some coastal zones of Greece, where the PoE has gone from moderate (yellow) to reasonable (orange). This is a substantial increment in the area with a reasonable likelihood of exceeding the limit value of the PM_{10} annual average. Most striking is the enlarged red areas around Romania's capital Bucharest and in Hungary. There the likelihood of exceedances increases from a reasonable to very likely, like at the Po-valley which is unchanged red. In these areas considerable reductions may be needed to reach non-exceedance levels in the future.

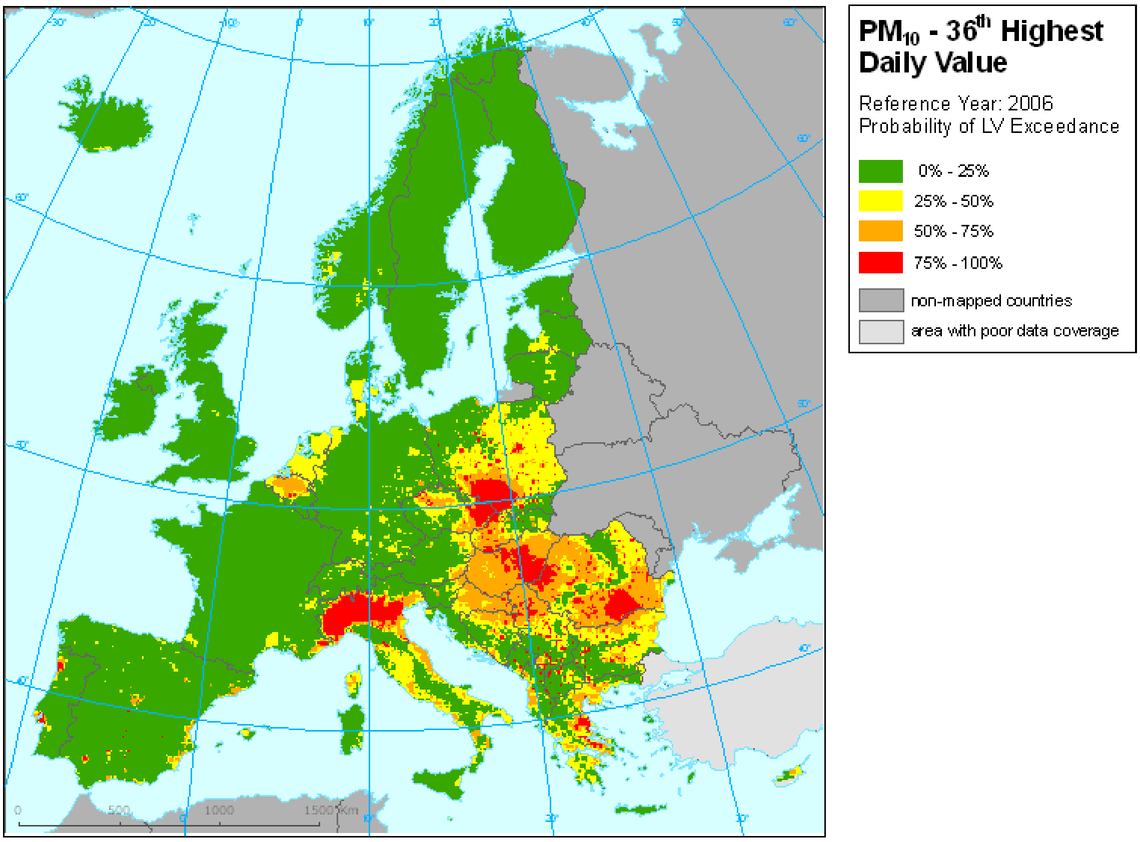

Figure 4.6 Map with the probability of the limit value exceedance for PM_{10} indicators 36^{th} maximum daily mean, in $\mu g.m^{-3}$ on the European scale in 2006 on the 10 x 10 km grid resolution. Interpolation uncertainty only is considered, no other sources of uncertainty.

5 Ozone maps

For ozone two health-related indicators, the 26th highest daily maximum 8-hour running mean and the SOMO35, and two vegetation-related indicators, the AOT40 for crops and the AOT40 for forests, are considered. The maps of health-related indicators are created using the combination of rural and urban areas as described in Chapter 2. They are presented in the EEA LAEA5210 10x10 km grid projection. The maps of vegetation-related indicators were created for rural areas only in a 2x2 km grid covering the same domain as the EEA LAEA5210 10x10 km grid. This higher resolution is to serve the needs of the EEA Core Set Indicator 005 on ecosystem exposure to ozone. A more in depth analysis on the multi-annual trends in ground level ozone concentrations over the past 10-15 years can be found in EEA (2009b).

5.1 26th highest daily maximum 8-hour average

5.1.1 Concentration map

The combined interpolated map for 26th highest daily maximum 8-hour average is created by combining the rural and urban maps according the criterion as described in Chapter 2 and in Horálek et al. (2007). Both rural and urban maps were created by combining the annual averages from the measured ozone concentrations with supplementary data in a linear regression model, followed by the interpolation of its residuals by ordinary kriging.

The supplementary data were used in accordance with the recommendations given by Horálek et al. (2008). The recommended supplementary data for rural areas are EMEP model output, altitude and surface solar radiation for rural areas, and EMEP model output, wind speed and surface solar radiation for urban areas. (The relevant linear regression submodels are identified as O.Ear and UO.Ewr respectively).

The estimated parameters of the linear regression models and of the residual kriging are presented in Table 5.1. Neither for rural, nor for urban areas solar radiation is statistical significant for 2006 data. Next to these parameters, also statistical indicators of both the linear regression models and the residual kriging are included in this table. The closeness of the regression relation, expressed as the R^2 and standard error, is of a slightly poorer level on 2006 data for both the rural and urban areas (adjusted R^2 is 0.40, resp. 0.43) compared to 2005, where the values were 0.45 and 0.51 respectively (Horálek et al. 2008, Tables A3.1, resp. A3.11). RMSE and MPE are the cross-validation indicators, showing the quality of the resulting map. The RMSE analysis and comparison with 2005 results is discussed in Section 5.1.3.

Table 5.1 Parameters of the linear regression models (c, a1, a2, ...) and of the ordinary kriging variograms (nugget, sill, range) - and their statistics - of ozone indicator 26th highest daily maximum 8-hour mean for 2006 in the rural (left) and urban (right) areas as used for final mapping i.e. linear regression model O.Ear (left), resp. UO.Ewr (right) followed by the interpolation on its residuals using ordinary kriging (OK, coded 'a').

linear regr. model + OK on its residuals	rural areas (O.Ear-a)	urban areas (UO.Ewr-a)
	coeff.	coeff.
c (constant)	43.16	50.75
a1 (EMEP model 2006)	0.64	0.66
a2 (altitude GTOPO)	0.01	
a3 (wind speed 2006)		-3.63
a4 (s. solar radiation 2006)	non significant	non significant
adjusted R^2	**0.40**	**0.43**
standard error [µg.m^{-3}]	**12.09**	**11.62**
nugget	66	60
sill	132	111
range [km]	150	100
RMSE [µg.m^{-3}]	**11.17**	**10.17**
MPE [µg.m^{-3}]	**0.24**	**0.02**

The final map is presented in Figure 5.1. The areas and stations in the combined map where the target value (TV) of 120 µg.m^{-3} is exceeded are coloured red and purple.

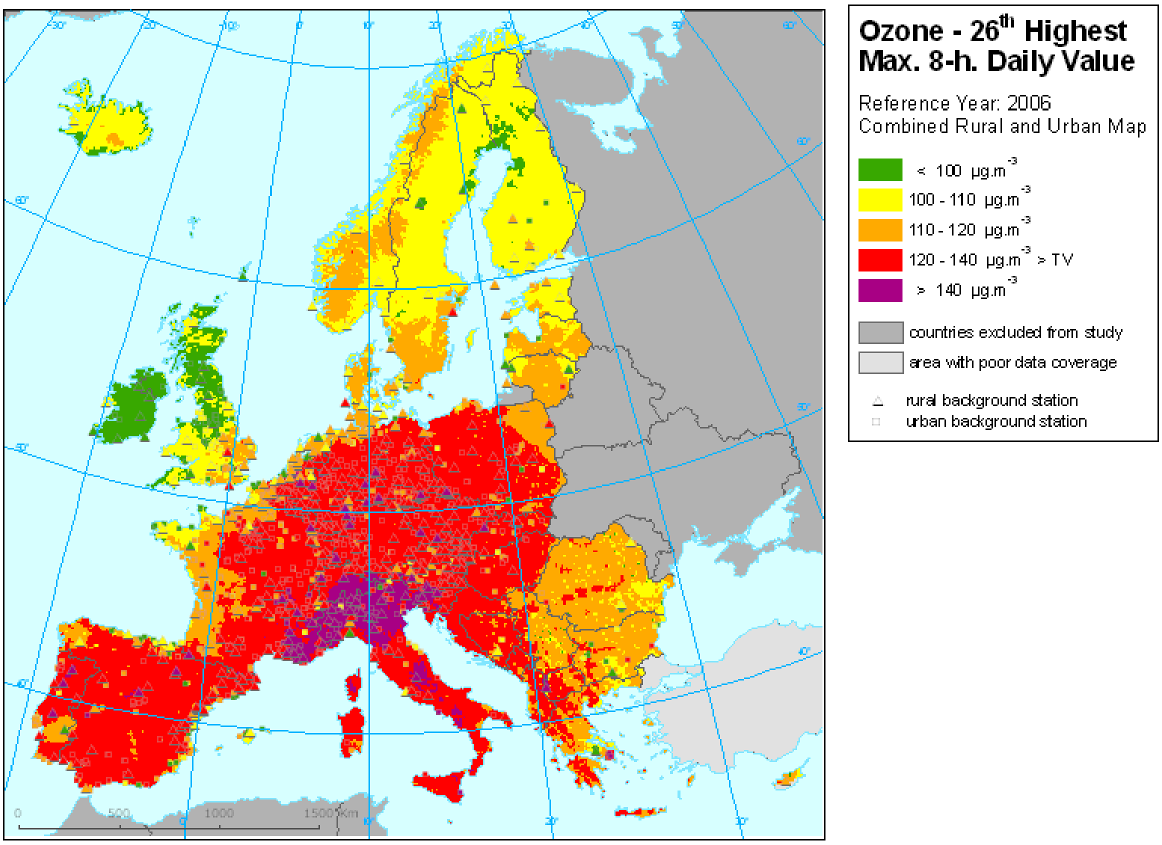

Figure 5.1 Combined rural and urban concentration map of ozone health indicators 26th highest daily maximum 8-hour value in µg.m^{-3} for the year 2006. Its target value is 120 µg.m^{-3}.

5.1.2 Population exposure

Table 5.2 gives for 26th highest daily maximum 8-hour mean the population frequency distribution for a limited number of exposure classes, as well as the population-weighted concentration for individual countries and for Europe as a whole.

Table 5.2 Population exposure and population weighted concentration – ozone, 26th highest daily maximum 8-hour mean for the year 2006.

Country	Population x1000	2006 Percent [%] < 100 µg.m-3	100 - 110 µg.m-3	(< TV) 110 - 120 µg.m-3	(> TV) 120 - 140 µg.m-3	> 140 µg.m-3	Population-weighted conc. [µg.m-3]
Austria	8217	0	0	4.6	93.7	1.7	127.6
Belgium	10594	1.9	0	3.1	95.0	0	126.1
Bulgaria	8011	18.0	31.8	48.6	1.6	0	107.9
Croatia	4400	0	0	11.3	88.2	0.6	126.3
Czech Republic	10163	0	0	1.4	98.6	0.0	127.5
Denmark	5423	1.2	50.7	47.8	0.3	0	108.6
Estonia	1364	2.0	88.3	9.6	0	0	106.4
Finland	5184	24.9	74.1	1.0	0	0	102.6
France	58437	1.1	6.1	28.4	62.3	2.1	122.7
Germany	82028	0.0	1.2	8.8	89.8	0.0	127.0
Greece	10876	0	18.4	42.5	38.6	0	117.3
Hungary	10125	0	0	14.8	85.2	0	123.4
Ireland	3734	99.4	0.6	0	0	0	91.3
Italy	56675	0	0.3	5.7	57.1	36.9	137.1
Latvia	2390	28.2	37.5	34.3	0	0	106.1
Liechtenstein	35	0	0	0	100.0	0	131.1
Lithuania	3479	0	40.9	59.0	0.0	0	110.6
Luxembourg	427	0	0	0	100.0	0	130.8
Malta	395	0	0	85.8	14.2	0	116.8
Netherlands	15746	6.4	17.9	37.4	38.3	0	116.1
Poland	38237	0.0	2.7	31.1	66	0	122.2
Portugal	9910	0.0	1.8	39.6	58.1	0	121.0
Romania	22341	15.8	32.9	49.9	1.3	0	108.1
San Marino	20	0	0	0	100.0	0	128.2
Slovakia	5295	0	0	13.6	86.4	0	124.6
Slovenia	2047	0	0	0.0	86.8	13	134.2
Spain	39046	3.2	20.2	26.5	50.0	0.1	118.0
Sweden	8898	7.4	56.6	35.7	0.3	0	108.1
United Kingdom	59051	57.3	36.0	6.7	0.0	0	98.8
Albania	3961	0	5.0	62.8	31.6	0.6	119.3
Andorra	61	0	0	66.7	33.3	0	123.7
Bosnia-Herzegovina	4203	0	10.6	38.7	50.7	0	119.8
Iceland	183	83.1	16.9	0	0	0	95.4
Macedonia, F.Y.R. of	2297	0	54.2	28.0	16.6	1.2	111.6
Montenegro	724	0	6.1	48.6	45.2	0	118.7
Norway	3226	17.1	77.2	5.7	0.0	0	103.1
Serbia	10821	11.2	36.0	44.0	8.8	0	110.5
Switzerland	7270	0.0	0.0	0.0	92	8	133.4
Total	**515294**	**9.8**	**14.2**	**20.5**	**51.0**	**4.5**	**119.6**
		44.5			**55.5**		

Note: Countries with the values based on ORNL population data with uncertain quality: AD, AL, BA, CH, IS, ME, MK, NO, RS. Countries with the lack of air quality or population density data are excluded from calculations in this paper: CY, TR.

It is estimated that about 55 % of the population lives in areas where the ozone target value (TV) of 120 µg.m^{-3} of the 26th highest daily maximum 8-hour mean is exceeded. However, as the current mapping methodology tends to underestimate high values, the percentage will most likely be even higher. Comparing with the 38 % of 2005 it demonstrates that 2006 shows a considerable increase of about 17 % in the population exposed to ozone levels above the TV. In general the frequency distribution shows a shift to increased higher class intervals in 2006 compared to 2005.

The overall European population-weighted ozone concentration in terms of the 26th highest daily maximum 8-hour mean in the background (neither hot-spot nor industrial) areas is estimated at almost

120 µg.m^{-3}, being around the target value. Compared to the 2005 results in Horálek et al. (2008) it is about 7 µg.m^{-3} higher in 2006.

5.1.3 Uncertainties

Uncertainty estimated by cross-validation

The basic uncertainty analysis is given by cross-validation. The absolute mean uncertainty of the map (using RMSE) in positions without measurement within the areas covered by measurements can be expressed in µg.m^{-3}. Table 5.1 shows RMSE values of 11.2 µg.m^{-3} for the rural areas and 10.2 µg.m^{-3} for the urban areas of the combined map. For the 2005 map the RMSE values were respectively 12.3 and 10.0 µg.m^{-3} (Horálek et al. 2008, Table A3.3 and A3.12), meaning the map for 2006 shows a lower absolute mean uncertainty at rural and a slightly higher absolute mean uncertainty at urban areas than at the map of 2005.

The relative mean uncertainty, being the absolute mean uncertainty value expressed as a percentage of the mean air pollution indicator value for all stations, of the map of ozone indicator 26th highest daily maximum 8-hour mean is 8.9 % for rural areas and 8.4 % for urban areas. These uncertainties are slightly lower, about 1.4 %, resp. 0.5 %, than the relative mean uncertainties of the 2005 map (10.3 % and 8.9 %).

Figure 5.2 shows the cross-validation scatter plots for both the rural and urban areas. The R^2 indicates that for the rural areas about 49 % and for the urban areas about 53 % of the variability is attributable to the interpolation. The values for the 2005 map were 51 % and 50 % respectively, showing a rather similar level of uncertainties for both the rural and urban interpolations at both years, despite the higher absolute ozone values in 2006.

The scatter plots of the interpolations show at areas with high values that the predictions lead here as well to an underestimation of the ozone indicator values at locations without measurements. For example, in the case of the rural map the value of 170 µg.m^{-3} would be estimated on average at about 150 µg.m^{-3} only, which is more than 10 % too low.

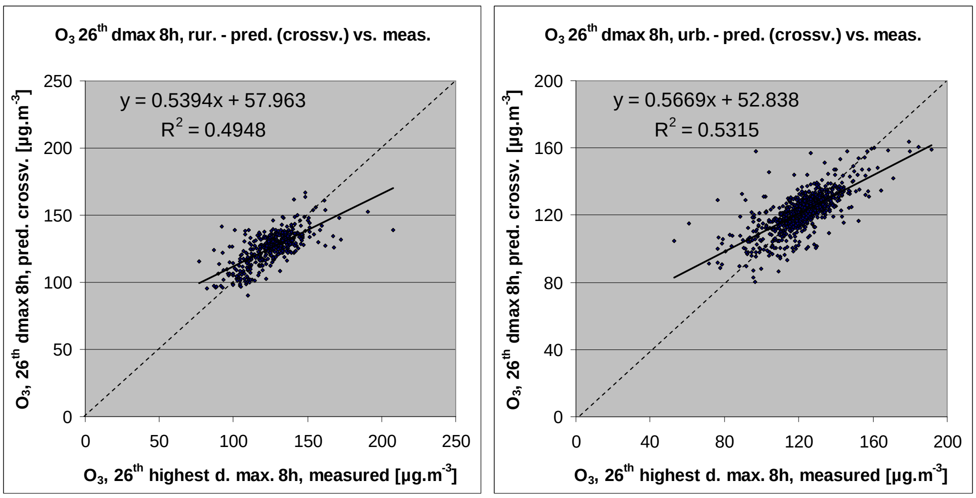

Figure 5.2 Correlation between cross-validation predicted values (y-axis) and measurements (x-axis) for the ozone indicator 26th highest daily maximum 8-hour mean for rural (left) and urban (right) areas in 2006.

Comparison of point measurement values with the predicted grid value

Additional to the cross-validation, a simple comparison between the measured and interpolated values averaged in a 10x10 km grid has been made. This point-grid comparison indicates to what extend the predicted value of a grid cell represents the corresponding measured values covered by that cell. The results of the cross-validation compared to this gridded validation examination are summarised in Table 5.3. The uncertainty at measurement locations is caused partly by the smoothing effect of interpolation and partly by the spatial averaging of the values in the 10x10 km grid cells. The level of smoothing leading to underestimation at high values is here smaller than it is at areas without measurement.

Table 5.3 Linear regression equation and coefficient of determination R^2 from the scatter plots of (i) the predicted point values based on cross-validation and (ii) aggregation into 10x10 km grid cells versus the measured point values for the ozone indicator 26th highest daily maximum 8-hour mean for rural and urban areas.

	rural areas		urban areas	
	equation	R^2	equation	R^2
i) cross-validation prediction	y = 0.539x + 57.96	0.495	y = 0.567x + 52.84	0.532
ii) 10x10 km grid prediction	y = 0.727x + 34.26	0.827	y = 0.727x + 32.90	0.799

Probability of target value exceedance map

Next to the cross-validation analysis and the comparison of predicted grid values with the points of measurement, the map with the probability of the target value exceedance has been constructed, using the concentration maps (Figure 5.1), the uncertainty map and the target value (TV), defined in the directive as 120 µg.m^{-3} for the 26th highest daily maximum 8-hour mean. The probability map is presented in Figure 5.3. Areas with the probability of limit value exceedance above 75 % are marked in red; areas below 25 % are marked in green. Areas with 25-50 %, resp. 50-75 % probability of TV exceedance are marked in yellow and orange. Section 4.1.3 explains in more details the significance of the colour classes in the map.

Comparing the 2005 with the 2006 probability of exceedance (PoE), most of the European area suffers from an increase in the PoE with a large area changing from a low (green), moderate (yellow) and reasonable (orange) into a considerable (red) likelihood of exceedance. The central-southern countries in Europe show unchanged high PoE (red). Whereas, the Iberian Peninsula, the Balkan countries and the south-eastern countries show decreases in the levels of PoE, meaning a reduced likelihood of exceeding target values.

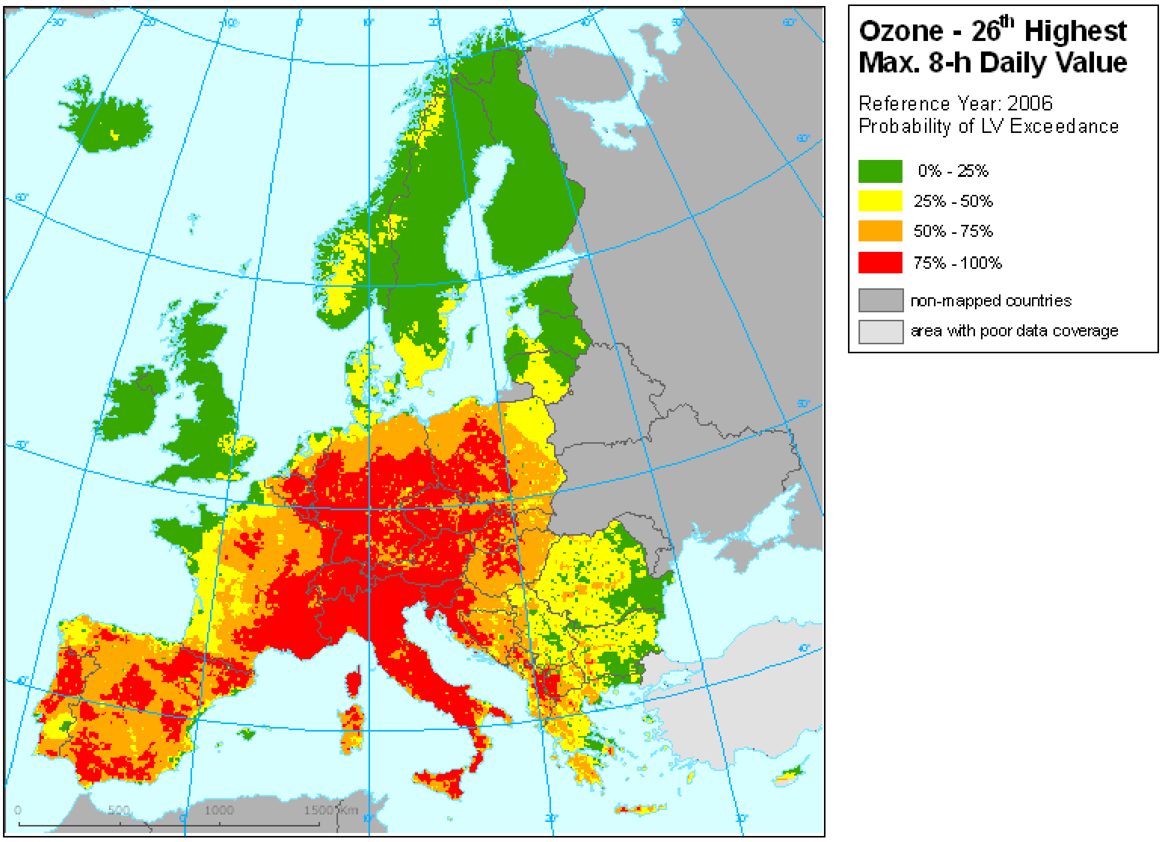

Figure 5.3 Map with the probability of the target value exceedance for ozone indicator 26th highest daily maximum 8-hour average values (in µg.m^{-3}) on European scale in 2006, 10 x 10 km grid resolution. Interpolation uncertainty only is considered, no other sources of uncertainty.

5.2 SOMO35

5.2.1 Concentration map

The combined interpolated map for SOMO35 is created by combining the rural and urban maps, according the criterion as described in Section 2 and in Horálek et al. (2007). Both rural and urban maps were created by combining the annual averages from the measured ozone concentrations with supplementary data in a linear regression model, followed by the interpolation of its residuals by ordinary kriging.

Like in the case of 26th highest daily maximum 8-hour mean, the recommended supplementary data (Horálek et al., 2008) for rural areas are EMEP model output, altitude and surface solar radiation for rural areas, and EMEP model output, wind speed and surface solar radiation for urban areas. (The relevant linear regression submodels are identified as O.Ear, resp. UO.Ewr.)

The estimated parameters of the linear regression models and of the residual kriging are presented in Table 5.4, including the statistical indicators. The closeness of the regression is shown by R^2 and standard error. The adjusted R^2 for the rural areas is 0.42 and for the urban areas 0.38, which is at a somewhat lower level than the adjusted R^2 values 0.51, resp. 0.49 of 2005 (Horálek et al. 2008, Tables A3.1, resp. A3.11). RMSE and MPE are the cross-validation indicators showing the quality of the resulting map of which the RMSE is discussed in more detail in Section 5.2.3.

Table 5.4 Parameters of the linear regression models (c, a1, a2, ...) and of the ordinary kriging variograms (nugget, sill, range) - and their statistics - of ozone indicator SOMO35 for 2006 in the rural (left) and urban (right) areas as used for final mapping, i.e. rural linear regression model O.Ear (left), resp. UO.Ewr (right) followed by the interpolation on its residuals using ordinary kriging (OK, coded with 'a').

linear regr. model + OK on its residuals	rural areas (O.Ear-a) coeff.	urban areas (UO.Ewr-a) coeff.
c (constant)	1500	1807
a1 (EMEP model 2006)	0.43	0.47
a2 (altitude GTOPO)	2.80	
a3 (wind speed 2006)		-257.82
a4 (s. solar radiation 2006)	108.11	81.58
adjusted R^2	**0.42**	**0.38**
standard error [μg.m^{-3}]	**2162**	**1622**
nugget	2.0E+06	1.1E+06
sill	3.8E+06	2.0E+06
range [km]	130	100
RMSE [μg.m^{-3}]	**2077**	**1471**
MPE [μg.m^{-3}]	**9**	**-3**

The final combined map is presented in Figure 5.4. SOMO35 is not subject to one of the EU air quality directives and no limit or target values have been defined, which does not offers the possibility to create a map with the probability of exceedances.

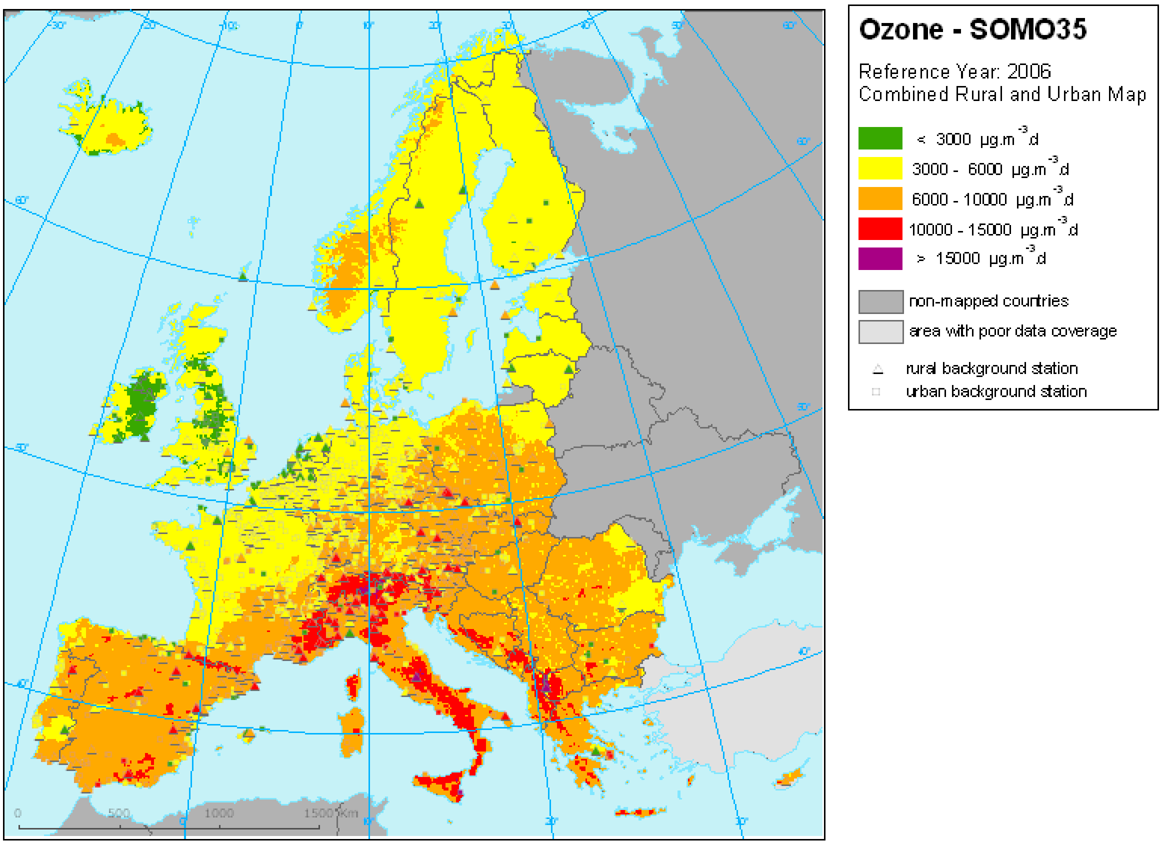

Figure 5.4 Combined rural and urban concentration map of ozone indicators SOMO35 in μg.m^{-3}.days for the year 2006.

5.2.2 Population exposure

Table 5.5 gives for SOMO35 the population frequency distribution for a limited number of exposure classes, as well as the population-weighted concentration for individual countries and for Europe as a whole.

Table 5.5 Population exposure and population weighted concentration – ozone, SOMO35, year 2006.

Country	Population	2006 Percent [%]					Population-weighted conc.
	x1000	< 3000 µg.m^{-3}.d	3000 - 6000 µg.m^{-3}.d	6000 - 10000 µg.m^{-3}.d	10000 - 15000 µg.m^{-3}.d	> 15000 µg.m^{-3}.d	µg.m^{-3}.d
Austria	8217	0	34.7	61.7	3.7	0.0	6975
Belgium	10594	1.9	97.7	0.5	0	0	4066
Bulgaria	8011	13.9	35.2	50.4	0.4	0	5611
Croatia	4400	0	4.7	94.5	0.8	0	7337
Czech Republic	10163	0	32.8	67.1	0.1	0	6471
Denmark	5423	3.7	96.3	0.0	0	0	4086
Estonia	1364	0	100.0	0	0	0	3837
Finland	5184	28.0	72.0	0	0	0	3454
France	58437	0.7	77.5	21.4	0.4	0	5117
Germany	82028	0.1	83.4	16.4	0.0	0	5104
Greece	10876	0	16.3	82.4	1.2	0	7020
Hungary	10125	0	36.6	63.4	0	0	6117
Ireland	3734	75.9	24.1	0	0	0	2598
Italy	56675	0	1.9	84.4	13.6	0.1	8678
Latvia	2390	23.9	76.1	0	0	0	4047
Liechtenstein	35	0	0	100.0	0	0	8179
Lithuania	3479	0	100.0	0.0	0	0	4678
Luxembourg	427	0	97.9	2.1	0	0	5279
Malta	395	0	0	100.0	0	0	7973
Netherlands	15746	35.8	64.2	0	0	0	3245
Poland	38237	0	55.5	44.5	0	0	5797
Portugal	9910	0	66.0	33.6	0.4	0	5534
Romania	22341	8.5	55.7	35.7	0.1	0	5330
San Marino	20	0	0	100.0	0	0	7841
Slovakia	5295	0	18.4	81.5	0.1	0	6967
Slovenia	2047	0	0	92.1	7.9	0	8124
Spain	39046	4.7	35.7	59.2	0.5	0	6174
Sweden	8898	6.0	94.0	0.0	0	0	4146
United Kingdom	59051	66.1	33.8	0.2	0	0	2799
Albania	3961	0	16.8	67.3	15.6	0.4	7632
Andorra	61	0	0	66.7	33.3	0	7872
Bosnia-Herzegovina	4203	0	29.5	63.8	6.7	0	7120
Iceland	183	69	30.6	0	0.0	0	2605
Macedonia, F.Y.R. of	2297	0	57.4	31.2	10.1	1.3	6627
Montenegro	724	0	31.9	51.6	16.5	0	7802
Norway	3226	28.1	68.8	3.0	0	0	3750
Serbia	10821	0	57.6	41.7	0.7	0	5724
Switzerland	7270	0	44.5	49.6	5.7	0.2	6701
Total	**515294**	**11.0**	**51.5**	**35.4**	**2.1**	**0.0**	**5485**
		62.6		**37.4**			

Note: Countries with the values based on ORNL population data with uncertain quality: AD, AL, BA, CH, IS, ME, MK, NO, RS. Countries with the lack of air quality or population density data are excluded from calculations in this paper: CY, TR.

It is estimated that about 37 % of the population live in areas with SOMO35 values above 6 mg.m^{-3}, which is compared to 2005 an increase of about 3 %, indicating the increasing ozone exposure in 2006.

The table shows that, compared to 2005, there is an overall increase in the number of inhabitants exposured to higher ozone concentrations according the SOMO35 indicator. In 2005 the exposure below 3 $mg.m^{-3}$ was some 25 % of all European inhabitants and in 2006 it has reduced to 11 %. Whereas the population exposure to values between 3 – 10 $mg.m^{-3}$ was some 71 % and has in considerably increased to 87 % in 2006, with however slightly reduced exposures from about 3.4 % in 2005 to 2.1 % in 2006 for values above 10 $mg.m^{-3}$.

This pattern can be derived also by comparing the 2005 with the 2006 map: Scandinavia and north-western Europe show a shift from a lower class interval to its neighbouring higher interval but hardly coming above the 6 $mg.m^{-3}$. An increased area of the mountainous area of Norway and the northern half of Poland and Germany do reach 6-10 $mg.m^{-3}$ whereas these areas did not have values between 3-6 $mg.m^{-3}$ in 2005. The Iberian Peninsula and a considerable part of the Balkan and Greece show decreased values going down from above 10 $mg.m^{-3}$ to values between 6 - 10 $mg.m^{-3}$. This tendency is reflected quite well by the shifts of the total population exposure percentages per class interval when comparing the 2005 values with those of Table 5.5 for 2006.

The total European population-weighted ozone concentration in terms of SOMO35 in the background (neither hot-spot nor industrial) areas is estimated as 5485 $\mu g.m^{-3}.d$. This is about 340 $\mu g.m^{-3}.d$ more than in 2005 (see Horálek et al., 2008) and confirms some overall increase in exposure from 2005 to 2006.

5.2.3 Uncertainties

Uncertainty estimated by cross-validation

The basic uncertainty analysis is given by cross-validation. The absolute mean uncertainty of the map, expressed by the RMSE, in positions without measurement within the areas covered by measurements can be expressed in $\mu g.m^{-3}.d$. In Table 5.4 the absolute mean uncertainty is 2077 $\mu g.m^{-3}.d$ for the rural areas and 1471 $\mu g.m^{-3}.d$ for the urban areas. The 2005 map shows a slightly higher value of 2173 $\mu g.m^{-3}.d$ for rural and about the same value (1459 $\mu g.m^{-3}.d$) for urban areas (Horálek et al. 2008, Table A3.4 and A3.13), meaning the map for 2006 differs with a slightly lower absolute mean uncertainty for the rural areas.

The relative mean uncertainty, being the absolute mean uncertainty value expressed as a percentage of the mean air pollution indicator value for all stations, of the map of ozone indicator SOMO35 is 31.6 % for rural areas and 29.2 % for urban areas. These uncertainties are slightly lower, about 3.9 %, resp. 3.2 %, than the uncertainties of the 2005 map.

Figure 5.5 shows the cross-validation scatter plots for interpolated values at both the rural and urban areas. The R^2 indicates that for the rural areas about 47 % and for the urban areas about 49 % of the variability is attributable to the interpolation. The values for the 2005 map were 55 % and 58 % respectively. Since the cross-validation RMSE of the interpolation is at both years of a reasonable similar level, the higher interpolation performance (higher R^2) at both the rural and the urban areas for 2005 is attributable to a better fitting linear regression model in 2005.

The scatter plots of the interpolations show again that at areas with high values the predicted values lead to a considerable underestimation of the ozone indicator at locations without measurements. For example, at the urban areas the value of around 12000 $\mu g.m^{-3}.d$ would lead on average to a predicted interpolation value of just above 8000 $\mu g.m^{-3}.d$ for such location without a station. This is about 33 % too low leading in general to high uncertainties at high SOMO35 values.

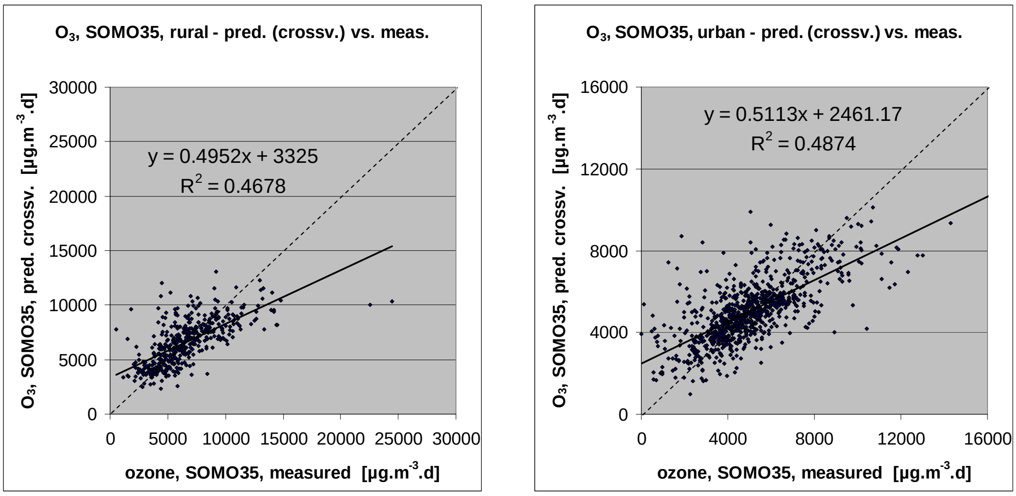

Figure 5.5 Correlation between cross-validation predicted values (y-axis) and measurements (x-axis) for the ozone indicator SOMO35 for rural (left) and urban (right) areas in 2006.

Comparison of point measurement values with the predicted grid value

Additional to the point cross-validation, a simple comparison between the point measured and interpolated values averaged in a 10x10 km grid has been made. This point-grid value comparison indicates to what extend the predicted value of a grid cell represents the corresponding measured station values covered by that cell. The results of the point cross-validation compared to this point-gridded validation examination are summarised in Table 5.6. The table shows a case ii) with better correlation between the station measurements and the interpolated values of the corresponding grid cells for both rural and urban areas (i.e. higher R^2, smaller intercept and a slope closer to 1) than it does at case i) the point cross-validation predictions of Figure 5.5. Case ii) represents the uncertainty in the predicted gridded interpolation map and the actual station measurements at the actual station location itself, whereas the cross-validation (case i)) simulates the behaviour of the interpolation at point positions without actual measurements within the area covered by measurements. The uncertainty at measurement locations is caused partly by the smoothing effect of the interpolation and partly by the spatial averaging of the values in the 10x10 km grid cells. The level of the smoothing effect leading to underestimation at high values is there smaller than it is at the areas without measurement.

Table 5.6 Linear regression equation and coefficient of determination R^2 from the scatter plots of (i) the predicted point values based on cross-validation and (ii) aggregation into 10x10 km grid cells versus the measured point values for the ozone indicator SOMO35 for rural and urban areas.

	rural areas		urban areas	
	equation	R^2	equation	R^2
i) cross-validation prediction	y = 0.495x + 3325	0.468	y = 0.511x + 2461	0.487
ii) 10x10 km grid prediction	y = 0.710x + 1912	0.837	y = 0.666x + 1680	0.771

No limit or target value is set for the WHO recommended ozone health indicator SOMO35, therefore no probability of exceedance map has been prepared.

5.3 AOT40 for crops and for forests

The ecosystem based accumulative ozone indicators described in this section are specifically meant for insertion in the EEA CSI005. For the estimation of the vegetation and forest land areas exposed in excess of the accumulated ozone, the maps in this section are created on a 2x2 km grid resolution instead the 10x10 km as used at the other indicators of this paper. This resolution is selected as a practical compromise in calculation time and accuracy in the impact analysis done for the EEA Core Set of Indicator 005 (CSI005; http://themes.eea.europa.eu/IMS/CSI). This CSI005 on ecosystem based ozone impact assessment uses the results of this section. This higher resolution is expected to provide some enhanced result in the overlay of the ozone indicator interpolated grids with the 250x250 meter grids of CLC2000 land cover map classes, due to a closer match between their grid resolutions, leading to some additional refinement in the exposure frequency distributions.

5.3.1 Concentration maps

The interpolated maps for AOT40 for crops and AOT40 for forests are created for rural areas only, using the combination of measured and supplementary data, as recommended in Horálek et al. (2008). The recommended supplementary data are the same as for the other ozone indicators: EMEP model output, altitude and surface solar radiation. (The relevant linear regression submodel is identified as O.Ear.)

The estimated parameters of the linear regression models and of the residual kriging are presented in Table 5.7, including their statistical indicators. The closeness of the regression is shown by R^2 and the standard error. The adjusted R^2 for the rural areas is 0.45 for the AOT40 for crops and 0.47 for AOT40 for forests, which indicates that the fit of the regression is at a somewhat lower level than for 2005 with its adjusted R^2 values 0.53, resp. 0.52 (Horálek et al. 2008, Tables A3.2). RMSE and MPE are the cross-validation indicators, showing the quality of the resulting map of which the RMSE is discussed in Section 5.2.3.

Table 5.7 Parameters of the linear regression models (c, a1, a2, ...) and of the ordinary kriging variograms (nugget, sill, range) - and their statistics - of ozone indicators AOT40 for crops (left) and for forests (right) for 2006 in the rural areas as used for final mapping, i.e. rural linear regression model O.Ear followed by the interpolation on its residuals using ordinary kriging (OK, coded with 'a').

linear regr. model + OK on its residuals	**AOT40 for crops (O.Ear-a)**	**AOT40 for forests (O.Ear-a)**
	coeff.	**coeff.**
c (constant)	5757	1212
a1 (EMEP model 2006)	0.89	0.41
a2 (altitude GTOPO)	9.67	13.12
a3 (s. solar radiation 2006)	611.5	935.9
adjusted R^2	**0.45**	**0.47**
standard error [μg.m^{-3}]	**8221**	**12203**
nugget	2.9E+07	8.6E+07
sill	6.0E+07	1.2E+08
range [km]	350	350
RMSE [μg.m^{-3}]	**7674**	**11990**
MPE [μg.m^{-3}]	**124**	**162**

The final map of AOT40 for crops is presented in Figure 5.6. The areas and stations in the map that exceed the target value (TV) of 18 000 μg.m^{-3}.h are marked in red and purple. The rural map, based on rural background station measurements only, is presented here as it considers here an indicator for vegetation exposure to ozone and it is assumed that there is no relevant vegetation in the urban areas.

The same is the case for forests for which the final rural map of AOT40 for forests is presented in Figure 5.7. However, for AOT40 for forests there is no TV defined.

Both maps show throughout Europe an overall increase in the levels of AOT40 with large areas in exceedance to the target value (red and purple), even extending into the UK and Norway where 2005 showed low values of below 6 000 μg.m^{-3}.h.

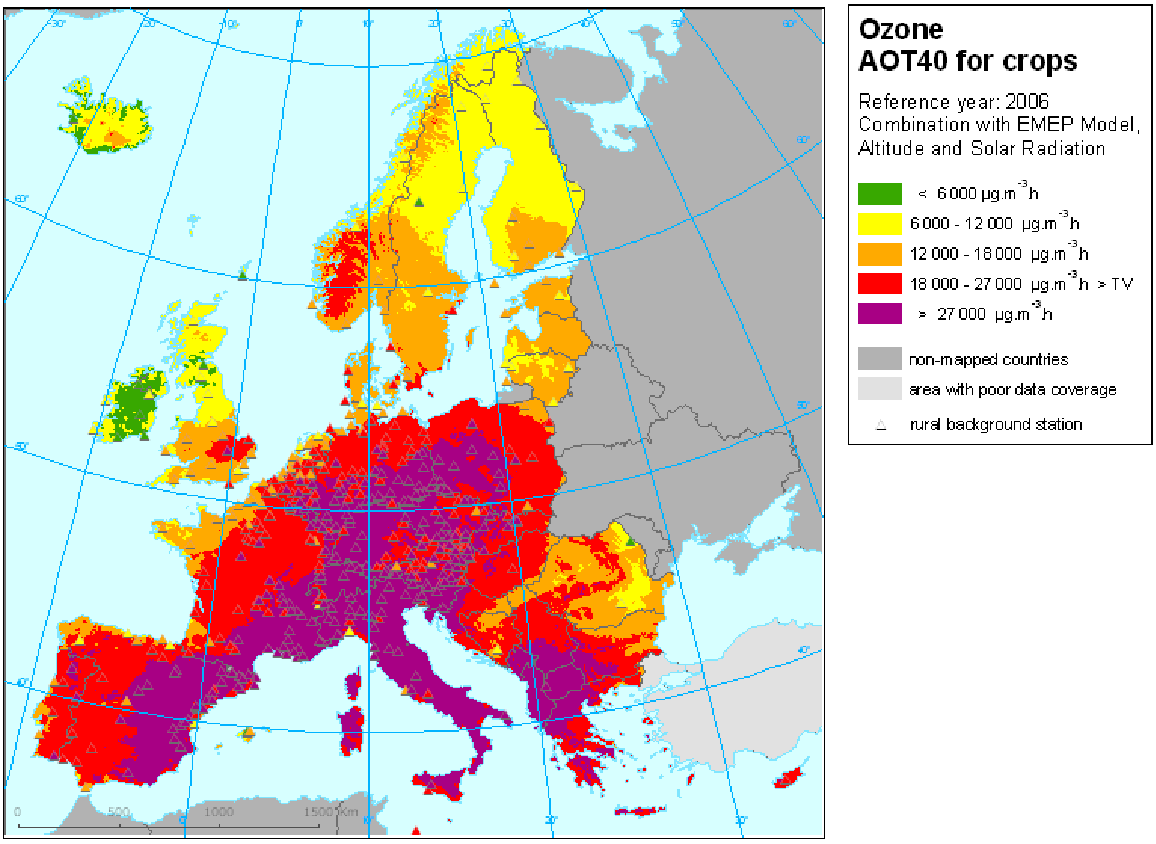

Figure 5.6 Rural concentration map of ozone vegetation indicator AOT40 for crops for the year 2006. Units: µg.m^{-3}.hours.

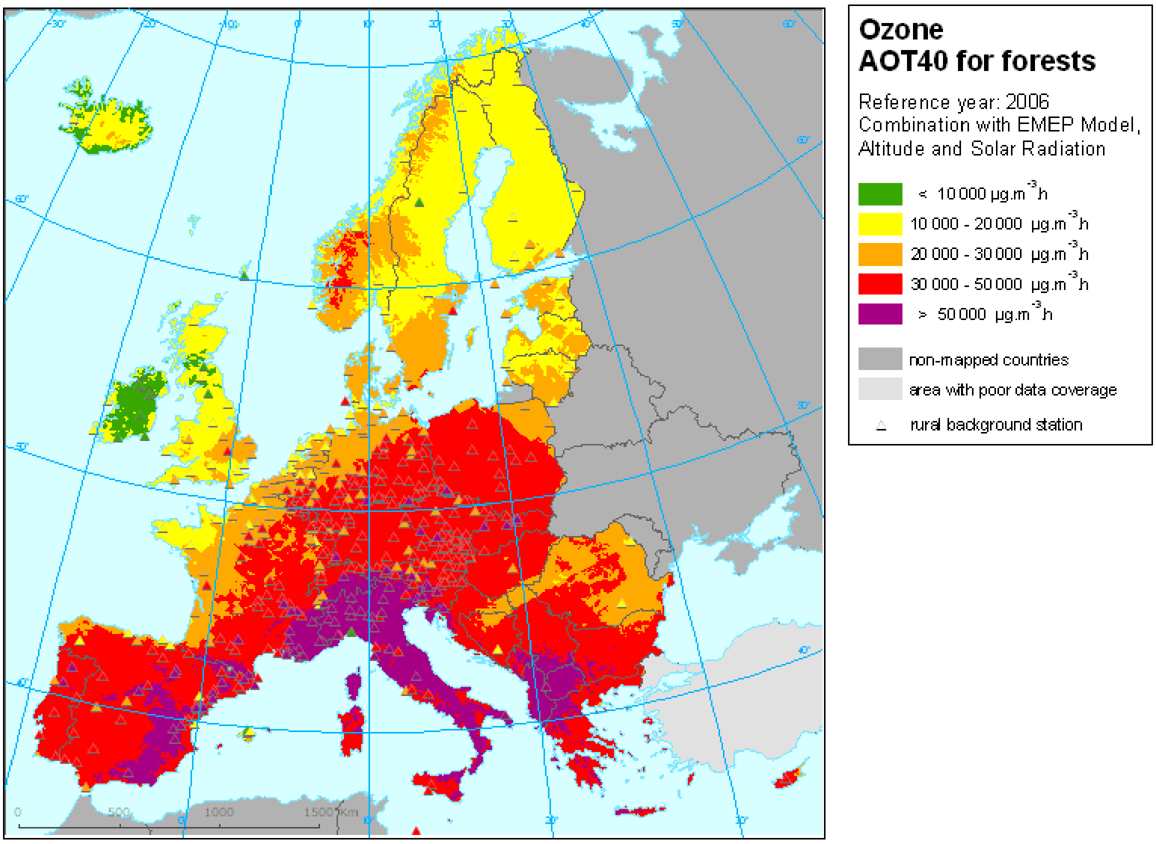

Figure 5.7 Rural concentration map of ozone vegetation indicator AOT40 for forests for the year 2006. Units: µg.m^{-3}.hours.

5.3.2 Vegetation exposure

Agricultural crops

The rural map with ozone indicator AOT40 for vegetation, i.e. agricultural crops, as given in Figure 5.6 has been combined with the land cover CLC2000 map. Following a similar procedure as described in Horálek et al (2007) the exposure of agricultural areas – defined as the Corine Land Cover level-1 class *2 Agricultural areas* (encompassing the level-2 classes *2.1 Arable land, 2.2 Permanent crops, 2.3 Pastures and 2.4 Heterogeneous agricultural areas)* – has been calculated at the country-level and summed to European totals. Table 5.8 gives the absolute and relative agricultural area for each country and for four European regions where the target value (TV) and long-term objective (LTO) for ozone are exceeded. Besides, it presents the frequency distribution of the agricultural area over the exposure classes per country and for Europe as a whole.

The table indicates the country grouping with corresponding colours of the region. *Northern Europe*: Sweden, Finland, Estonia, Lithuania, Latvia and Denmark. *North-western Europe*: United Kingdom, Ireland, the Netherlands, Belgium, Luxembourg and France north of 45 degrees latitude. *Central and Eastern Europe*: Germany, Poland, Czech Republic, Slovakia, Hungary, Austria, Liechtenstein, Bulgaria and Romania. *Southern Europe*: Albania, Bosnia-Herzegovina, France south of 45 degrees latitude, Portugal, Spain, Italy, San Marino, Slovenia, Croatia, Greece, Cyprus, F.Y.R. of Macedonia and Malta.

Table 5.8 illustrates that about 70 % of all agricultural land is exposed to ozone exceeding the target value (TV) of 18 mg.m^{-3}.h and about 98 % is exposed to levels in excess of the long-term objective (LTO) of 6 mg.m^{-3}.h. This is a substantial increase in the total area with agricultural crops considered to suffer from adverse effects to ozone exposure compared to 2005, where just about 50 % of agricultural land was exposed to ozone levels in excess of the target value and almost 90 % in excess of the long term objective.

Similar to 2005 is in the southern countries about the same area, 95 %, exceeding the target values. In northern Europe the ozone levels are below the target value for about 95 % of the agricultural area versus 100 % in 2005. In the north-western region the area exceeding the target value has become almost 50 % which is about four times larger than in 2005. For the central and eastern region the total exceeded area has increased considerably as well: from 44 % in 2005 to 77 % in 2006. Compared to 2005, the frequency distribution of agricultural area over the exposure classes shows for 2006 a clear shift towards higher exposures leading to an increased total area exceeded.

Table 5.8 Agricultural area exposure and exceedance (Long Term Objective, LTO, and Target Value, TV) for ozone, AOT40 for crops, year 2006.

Country	Agricultural Area, 2006					Percentage of agricultural area, 2006 [%]				
	total area	> LTO (6 mg.m-		> TV (18 mg.m-		< 6	6 - 12	12 - 18	18 - 27	> 27
	[km^2]	[km^2]	[%]	[km^2]	[%]	mg.m^{-3}.h	mg.m^{-3}.h	mg.m^{-3}.h	mg.m^{-3}.h	mg.m^{-3}.h
Albania	7183	7183	100	7183	100	0	0	0	0	100
Austria	27444	27444	100	27444	100	0	0	0	44.0	56.0
Belgium	17648	17648	100	17292	98	0	1.9	0.1	78.5	19.5
Bosnia-Herzegovina	19260	19260	100	12074	63	0	0.4	37.0	60.6	2.0
Bulgaria	57350	57350	100	25524	45	0	0.6	54.9	37.4	7.1
Croatia	24128	24128	100	19821	82	0	0	17.8	53.1	29.0
Cyprus	4287	4287	100	4244	99	0	0	1.0	89.9	9.1
Czech Republic	45546	45546	100	45546	100	0	0	0	30.6	69.4
Denmark (incl.	32235	32235	100	1694	5	0	0.5	94.2	5.3	0
Estonia	14678	14678	100	0	0	0	4.1	95.9	0	0
Finland	28829	28829	100	0	0	0	65.7	34.3	0	0
France	328462	328378	100	256159	78	0.0	2.4	19.6	59.1	18.9
Germany	213515	213515	100	202184	95	0	0.0	5.3	45.8	48.9
Greece	51546	51546	100	49095	95	0	0	4.8	61.6	33.6
Hungary	63069	63069	100	58894	93	0	0	6.6	87.5	5.8
Ireland	46385	10328	22	0	0	77.7	22.3	0	0	0.0
Italy	155631	155631	100	155627	100	0	0	0.0	9.4	90.6
Latvia	28296	28296	100	0	0	0	13.6	86.4	0	0
Liechtenstein	42	42	100	42	100	0	0	0	0	100
Lithuania	40021	40021	100	0	0	0	25.2	74.8	0	0
Luxembourg	1410	1410	100	1410	100	0	0	0	4.0	96.0
Macedonia	9514	9514	100	9514	100	0	0	0	0	100
Malta	124	124	100	124	99	0	0	0.7	99.3	0
Monaco	0	0	100	0	100	0	0	0	0	100
Netherlands	24894	24894	100	13276	53	0	10.6	36.1	52.7	0.6
Poland	200505	200505	100	189270	94	0	0	5.6	65.9	28.5
Portugal	42562	42562	100	37339	88	0	0.8	11.5	83.5	4.3
Romania	134906	134906	100	14023	10	0	21.8	67.8	10.4	0.0
San Marino	43	43	100	43	100	0	0	0	0	100
Slovakia	24342	24342	100	24127	99	0	0	0.9	74.1	25.0
Slovenia	7127	7127	100	7127	100	0	0	0	6.2	93.8
Spain	252334	252300	100	235401	93	0.0	1.4	5.3	50.7	42.6
Sweden	38617	38617	100	4872	13	0	11.6	75.8	12.6	0
United Kingdom	141984	128901	91	20455	14	9.2	36.7	39.7	14.4	0
Total	**2083917**	**2034659**	**98**	**1439803**	**69**	**2.4**	**7.0**	**21.6**	**40.9**	**28.2**
France over 45N	260757	260672	100	191280	73	0.0	3.0	23.6	63.1	10.3
France bellow 45N	67706	67706	100	64879	96	0.0	0.1	4.1	43.5	52.3
Northern	182675	182675	100	6566	4					
North-western	493078	443854	90	243713	49					
Central & eastern	773902	773902	100	594236	77					
Southern	634262	634228	100	595288	94					
Total	**2083917**	**2034659**	**98**	**1439803**	**69**					

Note: Countries not included due to lack of land cover data: AD, CH, IS, ME, NO, RS, TR.

Forests

The rural map with ozone indicator AOT40 for forests, as given in Figure 5.7 has been combined with the land cover CLC2000 map as well. Following a similar procedure as described in Horálek et al (2007) the exposure of forest areas – defined as the Corine Land Cover level-2 class *3.1. Forests* and *3.2 Scrub and/or herbaceous vegetation associations*, being two out of the three classes of the level-1 class *3. Forests and semi-natural areas* – have been calculated at the country-level.

Table 5.9 gives the absolute and relative forest area for each country and for four European regions where the – let us call it – *Reporting Value* (RV) of 20 mg.m^{-3}.h as Annex III of the ozone directive defines it, in combination with the *Critical Level* (*CL*) of 10 mg.m-3.h as defined in the Mapping Manual (UNECE, 2004) are exceeded. Furthermore, the table presents the frequency distribution of the forest area over the exposure classes per country and for Europe as a whole. The reporting value of the ozone directive (RV) is exceeded in almost 70 % of the European forest area, while in 2005 it was almost 60 %, meaning almost 10 % increase of area. The remaining quarter of the total European forested area that did not exceed the critical level of 10 $mg.m^{-3}.h$ in 2005, does it now in 2006, making about all forested areas exceeding the critical level of the AOT40.

As in 2005, the whole southern European region has AOT40 levels exceeding both the critical level and the reporting value. The central and eastern regions show increases also leading to 100 % exceedance of both thresholds. In the north-western region the area exceeding the critical level increases from 84 % in 2005 to practically the whole area (98 %) in 2006. The area above the reporting value creases there from 69 % in 2005 to 80 % in 2006. Specifically in the northern region of Europe the area in exceedance increased considerably in 2006: the area above the critical level enlarges from 40 % in 2005 to even 100 % in 2006 and for the reporting value from no exceedance in 2005 to 23 % in 2006. In comparison with 2005, the frequency distributions of the forested area over the exposure classes for 2006 show a clear shift to higher exposures, specifically for the areas which had the lowest values and values well above the reporting value in 2005.

Table 5.9 Forest area exposure and exceedance (critical level, CL, and reporting value, RV) for ozone, AOT40 for forests, year 2006.

Country	Area of forests, 2006					Percentage of wooded area, 2006 [%]				
	total area	> CL (10 mg.m^{-3}.h)		> RV (20 mg.m^{-}		< 10	10 - 20	20 - 30	30 - 50	> 50
	[km^2]	[km^2]	[%]	[km^2]	[%]	mg.m^{-3}.h	mg.m^{-3}.h	mg.m^{-3}.h	mg.m^{-3}.h	mg.m^{-3}.h
Albania	7777	7777	100	7777	100	0	0	0	2.5	97.5
Austria	37609	37609	100	37609	100	0	0	0.2	91.9	8.0
Belgium	6098	6098	100	6086	100	0	0.2	22.5	77.3	0
Bosnia-Herzegovina	22816	22816	100	22816	100	0	0	15.0	83.0	2.1
Bulgaria	34814	34814	100	34814	100	0	0	6.4	82.6	11.1
Croatia	20178	20178	100	20178	100	0	0	8.8	66.3	24.8
Cyprus	1553	1553	100	1553	100	0	0	5.2	83.8	10.9
Czech Republic	25504	25504	100	25504	100	0	0	0	100	0.0
Denmark (incl.	3697	3697	100	3389	92	0	8.3	90.7	0.9	0
Estonia	20778	20778	100	10932	53	0	47.4	52.6	0	0
Finland	193275	193275	100	4025	2	0	97.9	2.1	0	0
France	144830	144830	100	140475	97	0	3.0	27.6	54.6	14.7
Germany	103797	103797	100	103612	100	0	0.2	13.7	86.1	0.0
Greece	23590	23590	100	23590	100	0	0	0.4	61.1	38.5
Hungary	17349	17349	100	17349	100	0	0	1.6	98.4	0
Ireland	2911	1510	52	0	0	48.1	51.9	0	0	0
Italy	78783	78783	100	78783	100	0	0	0	11.7	88.3
Latvia	26958	26958	100	10745	40	0	60.1	39.9	0	0
Liechtenstein	62	62	100	62	100	0	0	0	86.4	13.6
Lithuania	18662	18662	100	10284	55	0	44.9	55.1	0	0
Luxembourg	904	904	100	904	100	0	0	0.1	99.9	0
Macedonia	8616	8616	100	8616	100	0	0	0	2.9	97
Malta	2	2	100	2	100	0	0	0	100	0
Monaco	1	1	100	1	100	0	0	0	0	100
Netherlands	3100	3100	100	2719	88	0	12.3	87.2	0.5	0
Poland	91821	91821	100	91821	100	0	0	17.3	82.7	0.0
Portugal	24308	24308	100	24308	100	0	0	1.5	98.1	0.4
Romania	69822	69822	100	68965	99	0	1.2	47.0	51.7	0.1
San Marino	6	6	100	6	100	0	0	0	0	100
Slovakia	19297	19297	100	19297	100	0	0	0	98.9	1.1
Slovenia	11470	11470	100	11470	100	0	0	0	74.3	25.7
Spain	91880	91880	100	91341	99	0	0.6	9.7	62.6	27.1
Sweden	249779	249779	100	77936	31	0	68.8	31.0	0.2	0
United Kingdom	19666	18358	93	2163	11	6.7	82.4	11.0	0	0
Total	**1381712**	**1379002**	**100**	**959130**	**69**	**0.2**	**30.4**	**17.6**	**40.5**	**11.3**
France over 45N	89512	89512	100	85629	96	0	4.3	32.5	60.8	2.4
France bellow 45N	55318	55318	100	54846	99	0	0.9	19.8	44.6	34.8
Northern	513149	513149	100	117312	23					
North-western	122191	119482	98	97499	80					
Central & eastern	407851	407851	100	406808	100					
Southern	338521	338521	100	337511	100					
Total	**1381712**	**1379002**	**100**	**959130**	**69**					

Note: Countries not included due to lack of land cover data: AD, CH, IS, ME, NO, RS, TR.

5.3.3 Uncertainties

Uncertainty estimated by cross-validation

The absolute mean uncertainty of the map, expressed by the RMSE of cross-validation, in positions without measurement within the areas covered by measurements can be expressed in µg.m^{-3}.h. In Table 5.7 the absolute mean uncertainty is 7674 µg.m^{-3}.h for the AOT40 for crops and 11990 µg.m^{-3}.h for the AOT40 for forests. In 2005 it was 7700 µg.m-3.h and 12500 µg.m^{-3}.h, showing the absolute uncertainty is about the same for both years.

The relative mean uncertainty, being the absolute mean uncertainty value expressed as a percentage of the mean air pollution indicator value for all stations, of the map of ozone indicator AOT40 for crops is about 30 % and of the map of AOT40 for forests about 34 %. These are considerably lower than those of the 2005 maps, where the relative mean uncertainties were 41 % for AOT40 for crops and 42 % for AOT40 for forests.

Figure 5.9 shows the cross-validation scatter plots of the AOT40 for both crops and forests. The R^2 indicates that for AOT40 for crops about 53 % and for AOT40 for forests about 49 % of the variability is attributable to the interpolation. The values for the 2005 maps were 56 % and 54 % respectively (Horálek et al. 2008, Tables A3.5 and A3.6), showing a lower level of performance for the interpolations in 2006, compared to 2005.

As at the previous ozone indicators already occurred, the cross-validation scatter plots show that at areas with high values there will be a serious underestimation of the predicted value at locations with no measurement. This can be reduced by extending the number of measurement stations and a more optimised spatial distribution of such stations especially at areas with such high values.

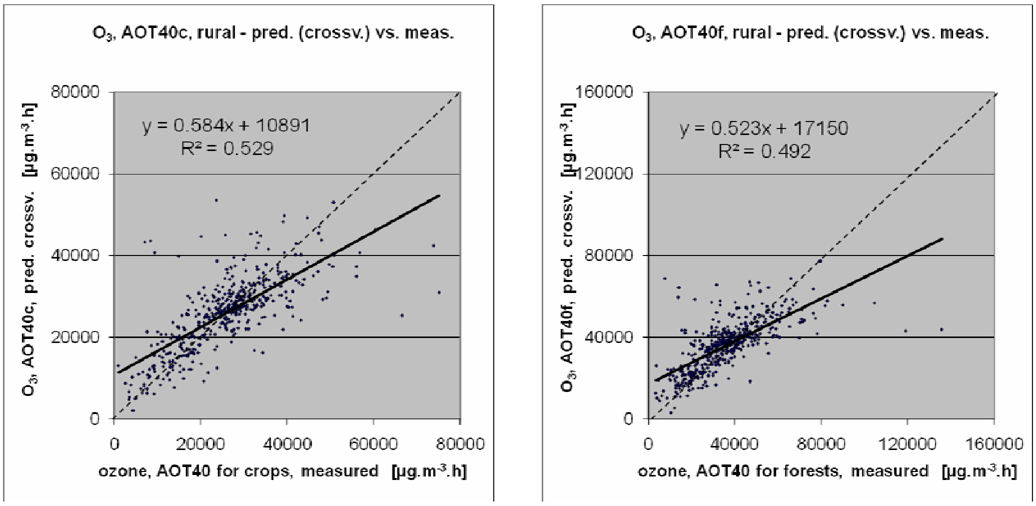

Figure 5.9 Correlation between cross-validation predicted values (y-axis) and measurements (x-axis) for the ozone indicators AOT40 for crops (left) and AOT40 for forests (right) for rural areas in 2006.

Comparison of point measurement values with the predicted grid value

Additional to the cross-validation, a simple comparison between the point measured and interpolated values averaged in a 10x10 km grid has been made. This point-grid comparison indicates to what extend the predicted value of a grid cell represents the corresponding measured station values covered by that cell. The results of the cross-validation compared to this point-gridded validation examination are summarised in Table 5.10. The table shows at case ii) a higher R^2 and a smaller intercept and a slope closer to 1 - indicating a better correlation - between the station measurements and the interpolated values of the corresponding grid cells for both rural and urban areas than it does at ii) the point cross-validation predictions of Figure 5.9. Case ii) represents the uncertainty in the predicted gridded interpolation map and the actual station measurements at the actual station location itself, whereas the cross-validation, case i), simulates the behaviour of the interpolation at point positions without actual measurements within the area covered by measurements. The uncertainty at measurement locations is caused partly by the smoothing effect of interpolation and partly by the spatial averaging of the values in the 2x2 km grid cells. The level of the smoothing effect leading to underestimation at high values is there smaller than it is at the areas without measurement.

Table 5.10 Linear regression equation and coefficient of determination R^2 from the scatter plots of (i) the predicted point values based on cross-validation and (ii) aggregation into 2x2 km grid cells versus the measured point values for PM_{10} indicator annual average for rural (left) and urban (right) areas.

	AOT40 for crops		AOT40 for forests	
	equation	**R^2**	**equation**	**R^2**
i) cross-validation prediction	y = 0.584x + 10891	0.529	y = 0.523x + 17150	0.492
ii) 2x2 km grid prediction	y = 0.724x + 7227	0.783	y = 0.629x + 13342	0.698

The AOT40 for crops with a target value of 18000 $\mu g.m^{-3}.h$ would allow us to prepare a probability of exceedance map. However, we limited the preparations involved with the accumulative ozone indicators to the specific needs of the EEA CSI005, not demanding such a probability of exceedance map.

6 Conclusion

Mapping and exposure results

The interpolated maps for 2006 on the PM_{10} and ozone human health related air pollution indicators are presented in this paper, together with their frequency distributions of the estimated population exposure and exceedances. It concerns the annual average and the 36^{th} maximum daily mean for PM_{10} and the SOMO35 for ozone. For ozone the interpolated maps on the ecosystem based indicators AOT40 for crops and AOT40 for forests are presented, including their frequency distribution of estimated land area exposures and exceedances.

PM_{10}

The number of Europeans exposed to annual mean concentrations of PM_{10} above the limit value (LV) of 40 $ug.m^{-3}$ is at least 8 % of the total population (Table 4.2). This is 1% lower then in the year 2005. The differences between these two years may be of no real significance when taking into account the uncertainties with which these numbers are surrounded. However, considering them in view of a multi-annual period they may be subject to a consistent downward trend. The number of Europeans exposed to concentrations even below 20 $\mu g.m^{-3}$ is also lower: 24 % in 2005 and 20 % in 2006. The number of people exposed to the concentrations between 20 and 40 $\mu g.m^{-3}$ rose from 67 % in 2005 to 72 % in 2006. It is estimated that the European inhabitants living in the background (neither hot-spot nor industrial) areas – without regard whether urban or rural – are exposed on average to the annual mean PM_{10} concentration of 27 $\mu g.m^{-3}$. In comparison with 2005 the European population weighted concentration, i.e. the average concentration per inhabitant taken for the whole of Europe, is about 1 $\mu g.m^{-3}$ higher in 2006, which can be considered about the same as in 2005.

At least 28 % of the European population lived in 2006 in areas where the PM_{10} limit value (50 $\mu g.m^{-3}$), of 36^{th} maximum daily mean is exceeded (Table 4.5). This percentage is similar to that of 2005. The overall European population-weighted concentration of the 36^{th} maximum daily mean for the background areas is estimated at about 45 $\mu g.m^{-3}$. Compared to 2005 this is just about 1.5 $\mu g.m^{-3}$ higher in 2006, which can be considered as being about a same level in both years.

One could conclude for PM_{10} in Europe that in general the PM_{10} indicators show slightly increased levels of exposure and exceedances in 2006 compared to 2005. There is some reduction in the number of inhabitants exposured to the lowest pollution classes, with a positive signal that the number of inhabitants exposed to the highest pollutant levels also have reduced slightly.

Ozone

For ozone indicator 26^{th} highest daily maximum 8-hour mean is estimated that at least 55 % of the population lives in areas where the ozone target value (TV) of 120 $\mu g.m^{-3}$ is exceeded (Table 5.2). Compared to 2005, 2006 shows a considerable increase of about 17 % in the population exposed to ozone levels above the TV. In general also the frequency distribution shows a shift to increased higher class intervals in 2006 compared to 2005. The overall European population-weighted ozone concentration in term of the 26^{th} highest daily maximum 8-hour mean in the background areas is estimated at almost 120 $\mu g.m^{-3}$. Compared to the 2005 results, this is about 7 $\mu g.m^{-3}$ higher in 2006.

It is estimated that about 37 % of the population live in areas with SOMO35 values above 6 $mg.m^{-3}$ (Table 5.5), which is an increase of about 3 % compared to 2005. The increase occurs specifically in areas of northern and north-western Europe where the lowest SOMO35 levels are found. Some limited reductions are found at Mediterranean countries. The overall European population-weighted ozone concentration in terms of SOMO35 in the background areas is estimated at 5485 $\mu g.m^{-3}.d$. This is about 340 $\mu g.m^{-3}.d$ more than in 2005, which confirms some overall increase in population exposure from 2005 to 2006.

About 70 % of all agricultural land is exposed to ozone exceeding the target value (TV of 18 $mg.m^{-3}.h$) for AOT40 for crops and about 98 % is exposed to levels in excess of the long-term objective (LTO) of 6 $mg.m^{-3}.h$ (Table 5.8). This is a substantial increase in the total area with agricultural crops considered to suffer from adverse effects from exposure to ozone compared to 2005. Then just about

50 % of agricultural land was exposed to ozone levels in excess of the target value and almost 90 % in excess of the long term objective.

For the ozone indicator AOT40 for forests, the reporting value of 20 $mg.m^{-3}$ is exceeded in about 69 % of the European forest area (Table 5.9), while this was only 59 % in 2005, showing a considerable increase.

The results in this report show that, generally over Europe, and most significantly over northern Europe, 2006 was characterised by higher ozone levels then in 2005. While the trends in mean ozone remain generally constant, there was a significant increase in 2006 in the averaged levels of accumulated ozone indicators SOMO35 and AOT40 for crops and forests.

Uncertainty results

Next to the creation of European wide interpolated air pollutant maps and exposure tables, the uncertainty of the presented maps is evaluated and maps of probability of limit value exceedance are estimated for the human health indicators.

The relative uncertainty of rural PM_{10} maps is about 27 % at both the annual average and the 36^{th} maximum daily mean. For the urban PM_{10} maps this is about 21 % for the annual average and about 23 % for the 36th maximum daily mean. The uncertainties are slightly higher than those of 2005; this is given probably by the poorer linear regression with supplementary data in 2006, compared to those of 2005.

The relative uncertainty of ozone maps is different for different indicators: for 26^{th} highest daily maximum 8-hour average it is about 9 % for rural areas and 8 % for urban areas; for SOMO35 it is about 32 % for rural and 29 % for urban areas. The relative uncertainty of rural AOT40 for crops map is 41 %, in the case of AOT40 for forests it is 42 %. The relative uncertainties are lower in comparison with 2005 results; contrary to this, the absolute uncertainties are higher – this is caused by the higher ozone concentrations in 2006.

The scatter plots of the interpolation results versus the measurements show that for both the PM_{10} and the ozone indicators in areas with high values, a systematic underestimation of the predicted values occurs, which leads to a considerable underestimation of the indicator values at locations without measurements. This effect is demonstrated most prominently at the ozone indicators. This underestimation would be reduced if a closer linear regression with (other) supplementary data would be reached. For example, in the near future more and more contribution from satellite imagery data and interpretation techniques may be expected. Other options are extending the number of measurement stations in general and optimising and extending monitoring networks. These perhaps based on alternative monitoring strategies and techniques and/or using additional mobile stations (in campaigns), which however are all expensive options.

Continued efforts aiming for a more optimised spatial distribution of (such) stations, especially in areas with high air pollution and reduction of external and interpolation uncertainties would definitely contribute to reduced uncertainties in the interpolations (see Denby et al. (2009).

Probability of exceedance

For both the human health indicators for PM_{10} and ozone, maps have been prepared showing the probability of the exceedance to the limit values or target values.

For the annual average PM_{10} the patterns in the spatial distribution of the different probability of exceedance (PoE) classes over Europe in 2006 do not differ much from those of 2005; just some enlargement and a shift from *moderate* to *reasonable* likelihood of exceedance in the isolated spots in the south-eastern countries of Europe, where a relatively limited number of measurement stations is located.

The 36th maximum daily means of PM_{10} do show in the south-eastern part of Europe considerable increases in the PoE for 2006, compared to those of 2005, going from *moderately* to even *considerable* likelihood. In these areas considerable reductions may be needed to reach non-exceedance levels in the future.

Comparing the 2005 with the 2006 probability of exceedance (PoE) for the ozone 26th highest daily 8-hour maximum average, most of the European area suffers from an increase in the PoE with a large area changing from a *low*, *moderate* and *reasonable* into a *considerable* likelihood of exceedance. The central-southern countries in Europe show unchanged high PoE, meaning exceedances are very likely. Whereas, the Iberian Peninsula, the Balkan countries and the south-eastern countries show decreases in the levels of PoE, meaning a reduced likelihood of exceeding target values.

References

AirBase, European air quality database, http://airbase.eionet.europa.eu

Cressie N (1993). Statistics for spatial data. Wiley series, New York.

De Leeuw (2009). Assessment of the health impacts of exposure to PM2.5 at a European level. ETC/ACC Technical Paper 2009/1 (in prep. To be published at http://air-climate.eionet.europa.eu/reports/ETCACC_TP_2009_1_HIA_PM2.5)

Denby B, Horálek J, Walker SE, Eben K, Fiala J (2005). Interpolation and assimilation methods for European scale air quality assessment and mapping. Part I: Review and recommendations. ETC/ACC Technical paper 2005/7. http://air-climate.eionet.europa.eu/docs/ETCACC_TechnPaper_2005_7_SpatAQ_Interpol_Part_I.pdf

Denby B, De Leeuw F, De Smet P, Horálek J (2009). Sources of uncertainty and their assessment in spatial mapping. ETC/ACC Technical Paper 2008/20. (http://air-climate.eionet.europa.eu/reports/ETCACC_TP_2008_20_spatialAQ_uncertainties)

EEA (2009a). Spatial assessment of PM_{10} and ozone concentrations in Europe (2005). EEA Technical report 1/2009. http://www.eea.europa.eu/publications/spatial-assessment-of-pm10-and-ozone-concentrations-in-europe-2005-1

EEA (2009b). Assessment of tropospheric ozone. An EEA Technical report x/2009. (in prep. To be published at http://www.eea.europa.eu/publications/

EMEP (2008). Transboundary Particulate Matter in Europe: Status Report 2008. EMEP Status Report 4/2008. http://www.emep.int/publ/common_publications.html

ECMWF: Meteorological Archival and Retrieval System (MARS). It is the main repository of meteorological data at ECMWF (European Centre for Medium-Range Weather Forecasts). http://www.ecmwf.int/.

Fagerli H, Simpson D, Tsyro S (2004). Unified EMEP model: Updates. In: EMEP Report 1/2004. MSC-W, Oslo, Norway. www.emep.int/publ/reports/2004/Status_report_int_del1.pdf

Horálek, J., Kurfürst, P., Denby, P., de Smet, P., de Leeuw, F., Brabec, M., Fiala, J. (2005). Interpolation and assimilation methods for European scale air quality assessment and mapping. Part II: Development and testing new methodologies. ETC/ACC Technical paper 2005/8. http://air-climate.eionet.europa.eu/docs/ETCACC_TechnPaper_2005_8_SpatAQ_Part_II.pdf

Horálek J, Denby B, de Smet PAM, de Leeuw FAAM, Kurfürst P, Swart R, van Noije T (2007). Spatial mapping of air quality for European scale assessment. ETC/ACC Technical paper 2006/6. http://air-climate.eionet.europa.eu/docs/ETCACC_TechnPaper_2006_6_Spat_AQ.pdf

Horálek J, de Smet PAM, de Leeuw FAAM, Denby B, Kurfürst P, Swart R, (2008). European air quality maps including uncertainty analysis. ETC/ACC Technical paper 2007/7. http://air-climate.eionet.europa.eu/reports/ETCACC_TP_2007_7_spatAQmaps_ann_interpol

Sandnes Lenschow H, Tsyro S (2002). Meteorological input data for EMEP/MSC-W air pollution models. EMEP MSC-W Note 2/2000. http://www.emep.int/publ/reports/2000/dnmi_note_2_2000.pdf

Simpson D, Fagerli H, Jonson JE, Tsyro S, Wind P, Tuovinen J-P (2003). Transboundary acidification and eutrophication and ground level ozone in Europe: Unified EMEP model description. EMEP Status Report 1/03 Part I. MNP, Oslo, Norway. http://www.emep.int/publ/reports/2003/emep_report_1_part1_2003.pdf

Tarrasón, L, Nyíri, Á. (2008). Transboundary acidification, eutrophication and ground level ozone in Europe in 2006. EMEP Status Report 1/2008. http://www.emep.int/publ/common_publications.html

Vestreng V, Mareckova K, Kakareka S,Malchykhina A, Kukharchyk T (2007). Inventory Review 2007; Emission Data reported to LRTAP Convention and NEC Directive, MSC-W Technical Report 1/07. http://www.emep.int/mscw/mscw_publications.html#2007

UNECE (2004). United Nations – Economic Commission for Europe, LRTAP Convention. Mapping Manual 2004. Manual on methodologies and criteria for Modelling and Mapping Critical Loads ands Levels and Air Pollution Effects, Risks and Trends. http://www.oekodata.com/icpmapping/htm/manual/manual_eng.htm